Project Report
ATC-221

Solid State Radar Demonstration Test Results at the FAA Technical Center

R. L. Ferranti

17 June 1994

Lincoln Laboratory
MASSACHUSETTS INSTITUTE OF TECHNOLOGY
LEXINGTON, MASSACHUSETTS

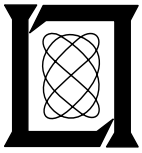

Prepared for the Federal Aviation Administration,
Washington, D.C. 20591

TECHNICAL REPORT STANDARD TITLE PAGE

1. Report No.	2. Government Accession No.	3. Recipient's Catalog No.

4. Title and Subtitle	5. Report Date
Solid State Radar Demonstration Test Results at the FAA Technical Center	17 June 1994
	6. Performing Organization Code
7. Author(s)	8. Performing Organization Report No.
Richard L. Ferranti	ATC-221
9. Performing Organization Name and Address	10. Work Unit No. (TRAIS)
Lincoln Laboratory, MIT P.O. Box 73 Lexington, MA 02173-9108	11. Contract or Grant No. DTFA01-93-Z-02012
12. Sponsoring Agency Name and Address	13. Type of Report and Period Covered
Department of Transportation Federal Aviation Administration Systems Research and Development Service Washington, DC 20591	Project Report
	14. Sponsoring Agency Code

15. Supplementary Notes

This report is based on studies performed at Lincoln Laboratory, a center for research operated by Massachusetts Institute of Technology. The work was sponsored by the Air Force under Contract F19628-90-C-0002.

16. Abstract

In 1992 and 1993 ITT Gilfillan teamed with Thomson CSF to develop a solid state transmitter system for airport surveillance radar applications. Because of the low peak power limitations of the solid state transmitter, the radar uses pulse compression techniques to obtain 55 nmi detection performance. In the Fall of 1992 ITT/Thompson executed a Cooperative Research and Development Agreement with the FAA's Terminal Area Surveillance System (TASS) program office to demonstrate the transmitter at the FAA Technical Center using the FAATC's ASR-9. The Laboratory participated in these tests, which were completed in April 1993.

The Laboratory test plan included an assessment of the solid state radar's time sidelobe levels, stability, susceptibility to short pulse interference, and target detection performance. Although the tests were limited in scope and the data required several post-collection processing corrections, the radar exhibited very low time sidelobe levels, had excellent stability, and showed adequate detection performance. The pulse compression receiver was vulnerable to short pulse interference and will require specialized processing techniques to minimize its effects.

It was not possible to take weather data, and the FAA Technical Center radar environment has no stressing clutter. Recommendations are made for the follow-on effort at a mountainous site to more completely characterize the solid state ATC radar.

17. Key Words		18. Distribution Statement
Airport surveillance radar	time sidelobes	This document is available to the public through the National Technical Information Service, Springfield, VA 22161.
solid state power amplifiers	radar stability	
pulse compression	radar interference	

19. Security Classif. (of this report)	20. Security Classif. (of this page)	21. No. of Pages	22. Price
Unclassified	Unclassified	46	

FORM DOT F 1700.7 (8-72) Reproduction of completed page authorized

EXECUTIVE SUMMARY

Though solid state radar has been used in military applications for many years, transistor power amplifiers capable of operating in the 2.9 GHz Air Traffic Control radar band have only recently become available. Solid state radar transmitters offer the potential for increased reliability and maintainability, and do not require the hazardous high voltages necessary for electron devices like klystrons. However, solid state transmitters cannot produce the high peak powers available from vacuum tubes, and use long coded pulses to obtain adequate detection performance. These pulse compression systems are new to primary air traffic control radar, and a number of technical issues such as the receiver's time sidelobes and its vulnerability to interference require investigation.

In 1992 and 1993 ITT Gilfillan teamed with Thomson-CSF to develop a solid state transmitter system for airport surveillance radar applications. The power amplifier was built by Gilfillan and the exciter/waveform generator and pulse compression receiver were developed by Thomson. The system uses a 75 microsecond nonlinear fm coded pulse, transmitted with a peak power of 22 kilowatts. For short range coverage, a 1 microsecond pulse is transmitted on another frequency.

In the Fall of 1992 ITT/Thomson executed a Cooperative Research and Development Agreement (CRDA) with the FAA's Terminal Area Surveillance System (TASS) program office to demonstrate the transmitter at the FAA Technical Center using the FAATC's ASR-9. The Laboratory participated in these tests, which were completed in April 1993.

The Laboratory test plan included an assessment of the solid state radar's time sidelobe levels, stability, susceptibility to short pulse interference, and target detection performance. A special-purpose doppler radar repeater was developed and fielded to perform some of these measurements. Although the tests were limited in scope, the radar exhibited very low time sidelobe levels (-55 dB to -51 dB, depending on target doppler), had excellent stability (62 dB, subject to post-collection data processing), and showed adequate detection performance at the short-pulse long-pulse transition range. The pulse compression receiver was vulnerable to short pulse interference and will require specialized processing techniques to minimize its effects.

Though generally favorable, the tests were not exhaustive because of the low clutter environment and lack of weather. In addition, the FAA Technical Center's standard ASR-9 does not support independent dual receive beams, which would have been a better match to the dual-pulse solid state radar. Hence, additional testing is recommended at a high-clutter site with a radar that has been modified to support dual beam receiving.

ACKNOWLEDGMENT

The author would like to thank John Maccini and Bob Kenney for fabrication and fielding of the radar repeater, Ken Saunders for assistance in its design, and Zahidul Hassan for his expertise in processing the data.

TABLE OF CONTENTS

LIST OF FIGURES

LIST OF FIGURES
(continued)

1. INTRODUCTION

This document summarizes the features, capabilities, and limitations of a solid-state S-band transmitter system built by ITT Gilfillan and Thomson-CSF and demonstrated under a Cooperative Research and Development Agreement (CRDA) with the Federal Aviation Administration's Terminal Area Surveillance System (TASS) program office. The transmitter system was installed at the FAA Technical Center (FAATC), and interfaced to a Westinghouse-built ASR-9 radar in the Fall of 1992, and was demonstrated and tested through April 1993. Testing was conducted by the FAATC, Lincoln Laboratory, and the Thomson/Gilfillan industrial partnership. The Laboratory-supervised test results are summarized here; results of the FAATC tests are being published separately [1].

The major purposes of the Lincoln Laboratory tests were to determine the radar system stability, the time sidelobe performance of the pulse compression waveform under a variety of conditions, and the system's detection performance, particularly at the crossover point between the short and long pulse waveforms. The Laboratory's evaluation was in general very favorable, although the tests were not exhaustive because of the low clutter environment near the Jersey shore and the lack of weather. In addition, the FAATC's standard ASR-9 does not support independent dual-beam low noise amplifiers (LNAs) and sensitivity time controls (STCs), which would have been a better match to the dual-pulse solid state radar. Recommendations are made for additional testing using a modified dual-beam ASR-9 in a severe clutter and weather environment.

2. SYSTEM CONFIGURATION

The solid state ASR transmitter system comprises three major components: the power amplifier, the receiver/exciter, and the data recorder. A block diagram of the solid state ASR transmitter system as configured at the FAA Technical Center is shown in Figure 1.

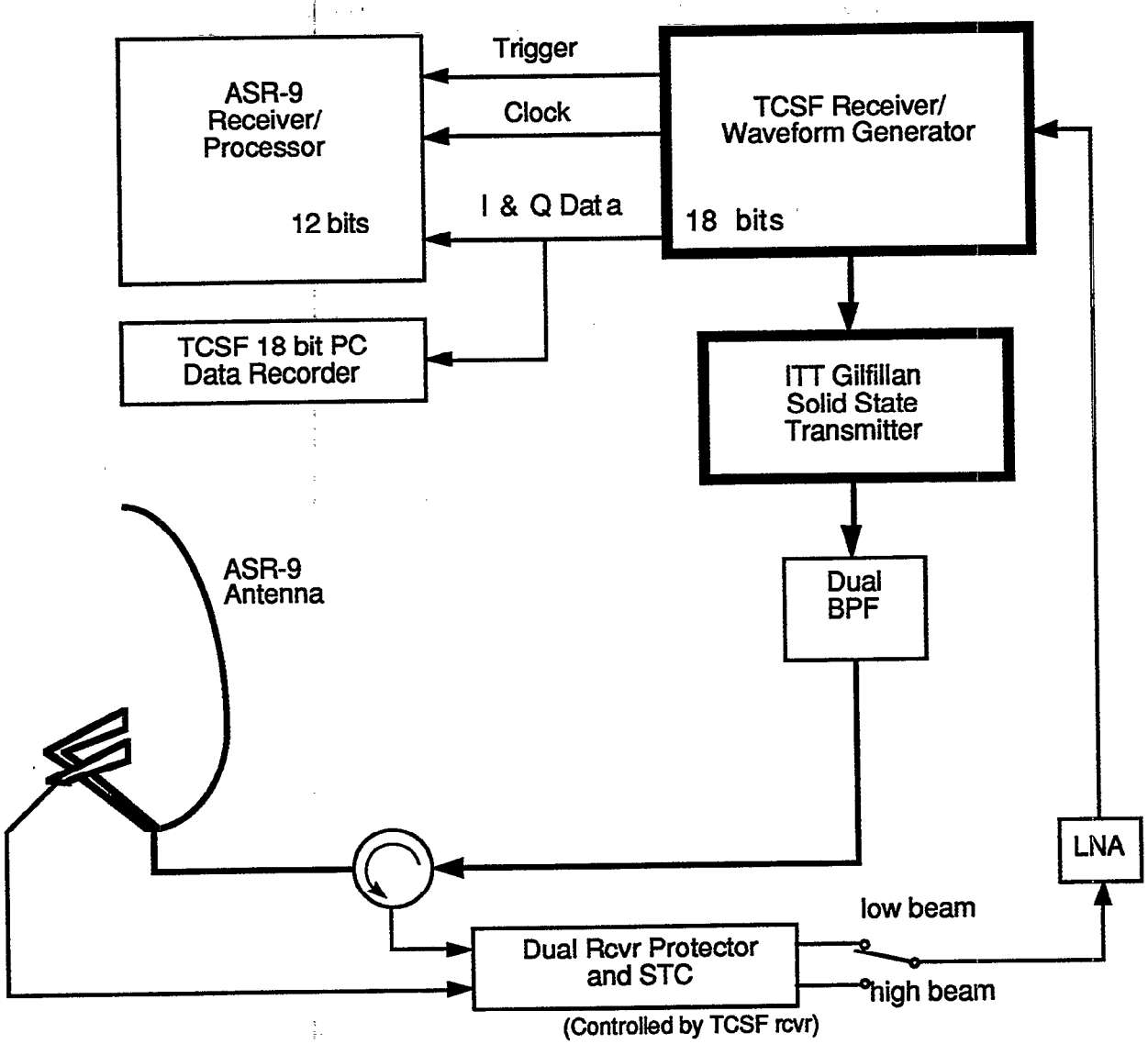

Figure 1. Solid State Radar Configuration at the FAATC ASR-9.

2.1 RF HARDWARE

The ITT Gilfillan power amplifier is a multistage design with a class A preamplifier feeding a class C driver, which in turn drives a 40-way power splitter and 40 power amplifier (PA)

modules. Output is taken from another 40-way combiner identical with (and built on the other side of) the input splitter. The preamp and drivers are redundant and automatically switch to the standby channel in case of a failure. The power amplifier is 40-way redundant; failure of any module results in graceful degradation of the output power. Any module may be replaced while the system is in operation. Up to three of the twelve current-sharing 43-volt switching power supplies may be removed and replaced without affecting transmitter power output. A photograph of the Gilfillan solid state power amplifier is shown in Figure 2. The power supplies are at the bottom, the driver stages are at the middle level, and the 40 output power modules are in the rotary configuration at the top. The amplifier is forced-air cooled.

The Thomson-CSF receiver/exciter comprises a nonlinear chirped digital waveform generator, a receiver switchable between the ASR-9 high and low beam horns with outputs for both the long and short pulsed waveforms, an offset–if sampling A/D converter, digital I & Q generation, pulse compression and compensation system, and an interface to the ASR-9 moving target detector (MTD) processor. The waveforms are a 75 microsecond nonlinear FM chirp followed by a 1-microsecond simple pulse, each transmitted on a different frequency. The time-bandwidth product of the chirped waveform is approximately 75; it chirps over a 1.25 MHz bandwidth.

2.2 DATA RECORDER

The Thomson-CSF radar data recording system is based on a custom Thomson interface coupled to a personal computer. Data from the interface are transferred to a computer parallel port and stored in memory to be later transferred to disk (internal or floppy).

Radar signals can be recorded from the short or long pulse prior to or after the amplitude/phase detection (I & Q data) and pulse compression (for the long pulse waveform). Indicator flags such as the reference clock, PRI trigger, CPI trigger, and azimuth reference pulse are also recorded. After pulse compression, each I & Q sample is 18 bits long.

The recorder's data buffer can be configured in a number of ways, for example, it could record two pulse-compressed CPIs (8/10 pulse bursts) over the radar instrumented range, or it could record a range/azimuth sector such as an area 4 nautical miles (nmi) by 12 degrees for every antenna scan. Selectable parameters include the range and azimuth extents, though both are bounded by the approximate magnitudes in the examples noted.

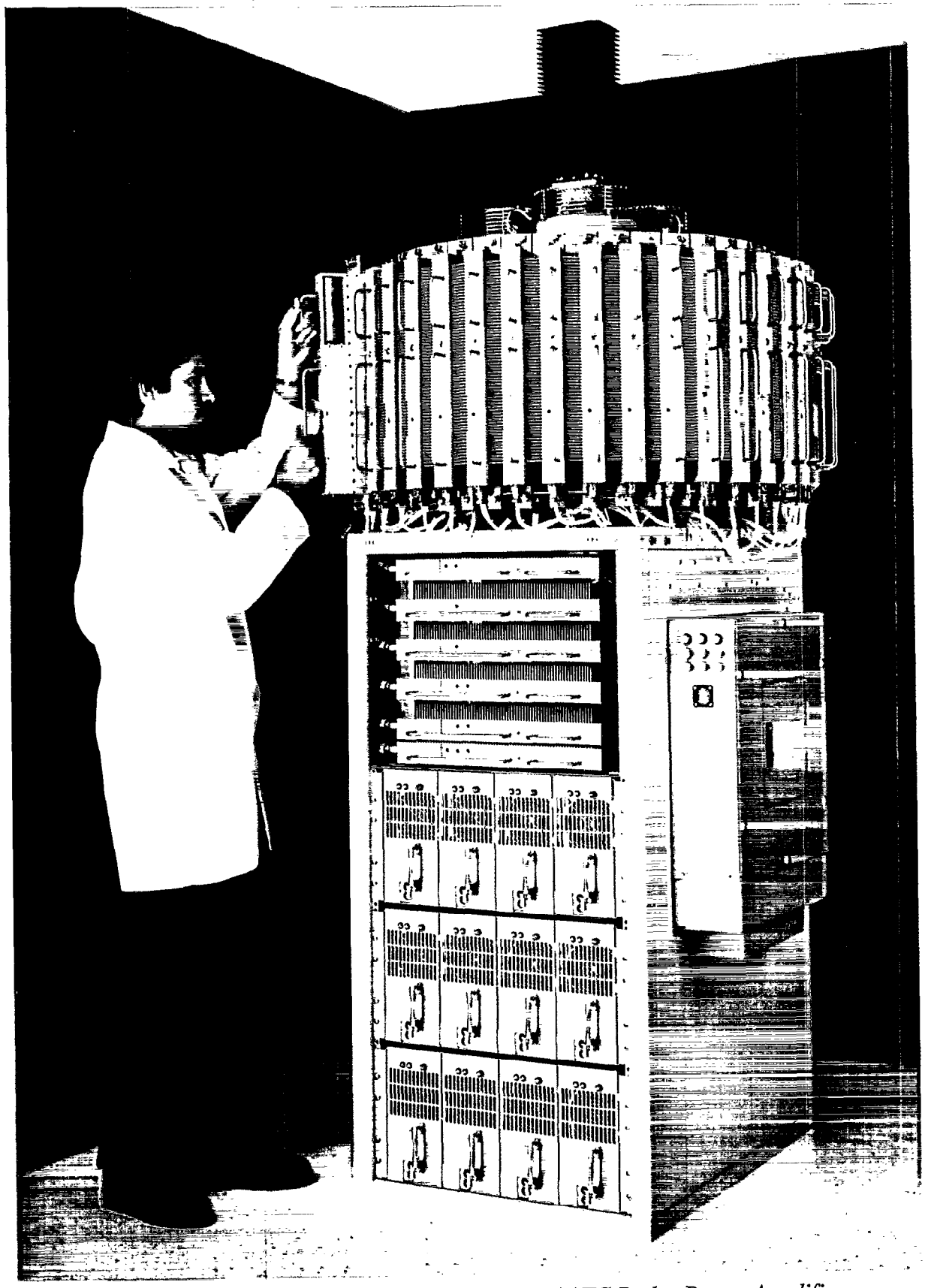

Figure 2. ITT Gilfillan Solid State S-band ATC Radar Power Amplifier.

3. TEST PLANS

Each organization involved with the solid state transmitter demonstration (the FAA Technical Center, ITT Gilfillan, Thompson CSF, and Lincoln Laboratory) submitted a test plan. The Laboratory test plan is summarized in the next section. The other tests plans included basic radar parameter measurements (transmitter power output, waveform characteristics, spectrum, receiver dynamic range, noise figure, bandwidth, I & Q balance) and detection performance against a variety of aircraft flown at different altitudes. A summary of these test results are included in the Appendix and are given in much more detail in the final FAATC report.

3.1 LINCOLN LABORATORY TEST PLAN

3.1.1 Stability

3.1.1.1 Measurement Technique

The measurement of radar system stability is a challenging task. Stability should always be measured with a relatively long time delay inserted between the transmitter and the receiver, because otherwise the radar's phase noise sources will be correlated, and the measurement will significantly underestimate the instability residue. Long delays are difficult to obtain microwave frequencies, and up/down conversion to a lower frequency convenient for bulk delay devices can contaminate the measurement with local oscillator phase noise from the test set. The best way to obtain long delays is to use a radar repeater located several miles from the system under test. In this case, the repeater must be stable enough not to corrupt the measurement (for modern high-stability radars, this means that the repeater must not use frequency conversion), the repeater must have sufficient power to drive the radar receiver to near saturation and significantly overcome returns from the surrounding ground clutter, and interference must be minimized both in the repeater design and in the subsequent data processing.

The radar stability measurement comprises recording complex samples of the repeated radar return, processing the data in the time and frequency domains to reject interference, and computing the ratio of the power of deterministic component of the repeated signal to the power of its noise components.

3.1.1.2 Repeater Description

The radar repeater used for stability assessment of the Gilfillan/Thomson solid state radar was designed to provide very clean, high-level signals at ranges of approximately 10 to 20 miles from the radar. It has two modes of operation; one is as a straight-through amplifier (yielding a return that appears to be a strong stationary point clutter source), and the other is as a moving target simulator (MTS). When in MTS mode, the repeated signal appears as a strong target moving at the maximum unambiguous velocity of the radar. It accomplishes this effect by applying a 180 degree phase reversal to every other repeated pulse. This feature is useful for stability measurements in presence of strong local ground clutter, as the signal appears in the part of the radar's doppler space farthest from the clutter return.

A block diagram of the repeater is shown in Figure 3. Straight-through amplification in the repeater is implemented by a low-noise amplifier with approximately a 2-dB noise figure driving a 1-watt power amplifier. The repeater front-end is protected from nearby radar interference by a

multipole cavity filter and a limiter. Radar signals are received and transmitted through stacked multielement Yagi antennas with about 22 dBi of gain. Yagi antennas were chosen because of their compact size and light weight; horn antennas with the same gain and beamwidth would have been prohibitively heavy and large.

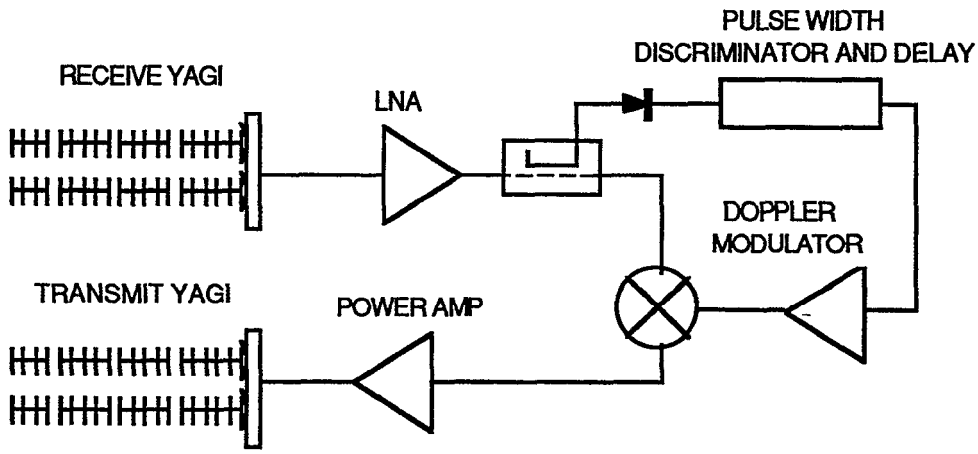

Figure 3. Moving Target Simulator Block Diagram.

When employed as a moving target simulator, the repeater samples the received pulses from the host radar and triggers a digital delay circuit. After about 100 microseconds (well past the time when the 75-microsecond radar pulse has been repeated), the delayed trigger inverts the polarity of a current, driving a mixer placed in the repeater signal path. The mixer, acting as a biphase modulator, changes the phase of the next received pulse by 180 degrees. Since the radar's pulse repetition interval is about 1 millisecond, the phase modulator has ample time to settle before the next pulse is received. The process repeats for each subsequent pulse, accomplishing the desired alternating pulse phase inversion. The advantages of this system are that no local oscillators are used in the repeater, spurious modulation is minimized because the modulator changes state between pulses, and amplitude/phase imbalances between the two modulator states affect only the carrier balance (zero doppler or clutter line) of the received signal.

It is important that the repeater's trigger circuit not be tripped by interference from other (short pulse) radars; to discriminate against short pulses the trigger circuit was designed with long time constants. The narrowband front-end filter also minimizes false triggering.

One of the keys to a successful field experiment is to give the field crew as much situational awareness as possible, such as a direct means of knowing that the field equipment is adjusted, oriented, and operating properly. In the MTS, the square-wave current drive to the biphase modulator is loosely coupled to an outboard battery-powered audio amplifier. When the repeater is operating properly, a pure tone at half the radar's PRF is heard. The tone will sound broken if the repeater is not reliably triggering on the radar signal because, for example, the receive antenna is not pointed right at the radar. The audio amplifier can also be unplugged from the MTS and a simple dipole/Schottky diode video radar detector substituted at the amplifier's input jack.

By swinging this "repeater detector" in front of the transmit antenna the operator can hear detected radar pulses and ascertain that *rf* energy is indeed being transmitted, confirming that the radar repeater is operating properly.

3.1.1.3 Measurements

Two main types of measurements were made. These were:

1. Loop tests (radar exciter output coupled to receiver input), with and without the repeater placed in the loop. This measurement confirms that the repeater's added phase noise is sufficiently low to allow a meaningful stability measurement. It also shows which power line-related spurious or other coherent signals can be attributed to the radar system and which are due to the repeater. Both constant pulse repetition frequency (PRF) and staggered PRF data were taken.
2. Field tests. The radar repeater was located approximately 10 miles away from the radar under test, at the site of an ARSR-2 enroute facility. The repeater operated from local power and was placed on a tower approximately 50 feet above ground level, inside the ARSR-2 radome. The ARSR-2 antenna was not rotating during the measurements. Measurements were made with the ASR-9 antenna halted and staring at the repeater, using fixed and staggered PRF's. No data were taken while the ASR-9 was antenna scanning since the repeater could not be located with the limited data acquisition/display capabilities of the Thomson demonstration computer.

3.1.1.4 Data Processing

The objective of this series of measurements was to assess the inherent amplitude and phase instability of the radar transmitter/receiver system. As in any measurement, and in particular for a field measurement, the data can be corrupted by a number of sources. These include power-line related spurious signals, interference from nearby emitters, imbalances and spurious modulation imposed by the radar repeater, and deterministic amplitude and/or phase modulations imposed by the transmitter. Each of these undesired signals will be removed by the following data processing techniques.

The first data-processing procedure is to remove line-type spectral components due to prime-power harmonics or sub-harmonics. The procedure is applied to constant PRF data; staggered PRF data require different processing described below. The 1024-pulse constant PRF data are first transformed to the frequency domain, where spurious lines are identified and excised. The excision replaces the amplitude/phase data associated with the particular line with an averaged value based on the noise level of the adjacent frequency bins. The data are then inverse transformed back to the time domain, and again transformed to the frequency domain to check that the spectrum has not been corrupted by the editing procedure.

Depending on the particular data, other spurious components are removed from the power spectrum. These components may include moving targets in the range cell (even at 3 a.m. when the field data were taken), or low-level spurious noise from the doppler modulator in the MTS. In general, these components were removed in the frequency domain, with an inverse transform and then another transform back into the frequency domain to ensure that the underlying noise and zero-doppler clutter data have not been affected.

A final source of interference is pulse-type noise either from a neighboring radar (such as the magnetron-based WSR-57 weather radar a few hundred feet from the ASR-9), or from stuck bits in the Thomson analog-to-digital converter. These outliers are easily found in the time domain data, and are edited to an average level corresponding to the data points in the vicinity. Very few such bad data points (about 2) are present in a 1024-point data set, however, they act like time-domain impulse functions and can noticeably raise the average noise level of the spectrum, particularly when that noise level is already 90 dB below the carrier. A typical before/after power spectrum for constant PRF (1000 Hz) data from the repeater is shown in Figure 4. Frequency domain data from an MTS test are shown in Figure 5 (the plus or minus 1/2 PRF lines from the MTS modulator are moved to zero doppler by the processing).

For staggered PRF data, frequency domain editing is not appropriate because of the limited resolution of the 8/10 pulse transforms. Time domain data processing is required and is complicated by the deterministic amplitude and/or phase modulations imposed by the transmitter. The modulation source is due to the thermal time constants of the transistors in the Gilfillan transmitter. There are short-term and long-term effects from this thermally-induced modulation. During the 75-microsecond pulse, the transmitter output droops in amplitude and imposes a nonlinear phase change on the transmitted signal. The Thomson pulse compression system compensates for this effect.

A constant PRF waveform needs no further compensation; however, the staggered ASR-9 PRFs introduce different duty cycles and therefore different long-term thermal effects. The primary effect is a exponential-like amplitude rise and fall during the 8 and 10 pulse sequences. A secondary effect is a step phase change during each pulse group. Since both these effects are deterministic and could be removed by the signal processor (as Thomson did for the short-term thermal effects), the stability measurement calculation for the staggered PRF waveforms considers only random phase and amplitude variations. The data processing procedure to remove the staggered PRF thermal effects is to fit a function of the form

$$A_0 + A_1*\mathrm{Cos}((\mathrm{pi}*(n-1)) + Bn + Cn^2 + Dn^3$$

to the amplitude and phase of each of n pulses in a 8 or 10 pulse group. The first term corrects for DC offsets (due to amplitude imbalance in the repeater's biphase modulator), the cosine term removes the biphase modulation from MTS data, and the linear, quadratic, and cubic terms perform an approximately exponential fit to the average value of the n data points. For the non-doppler data, the amplitude of the time series is corrected with a cubic fit with the A_1 term set to zero; phase correction is performed with a linear fit only (A_1, C, and D are set to zero). For doppler data, amplitudes were corrected with a quadratic fit and phase with a linear fit, with A_1 set to unity to remove the doppler modulation. An example of pre- and post-data processing for staggered PRF amplitudes is shown in Figure 6. Note that the data processing removes the long-term modulations due to interference sources (clutter movement, etc.) while preserving the noise-like pulse-to-pulse variations associated with the radar's instability residue.

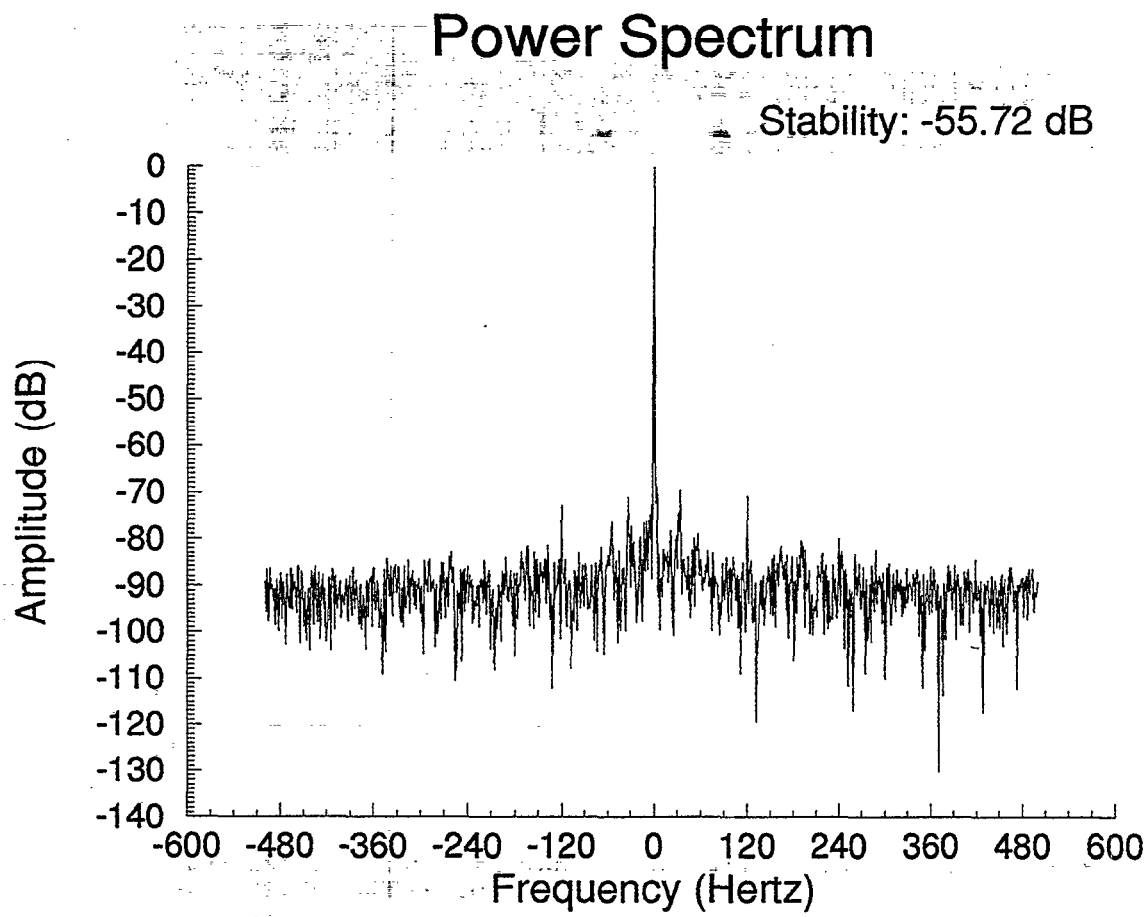

Figure 4a. Field Test: Raw MTS Data (no Doppler).

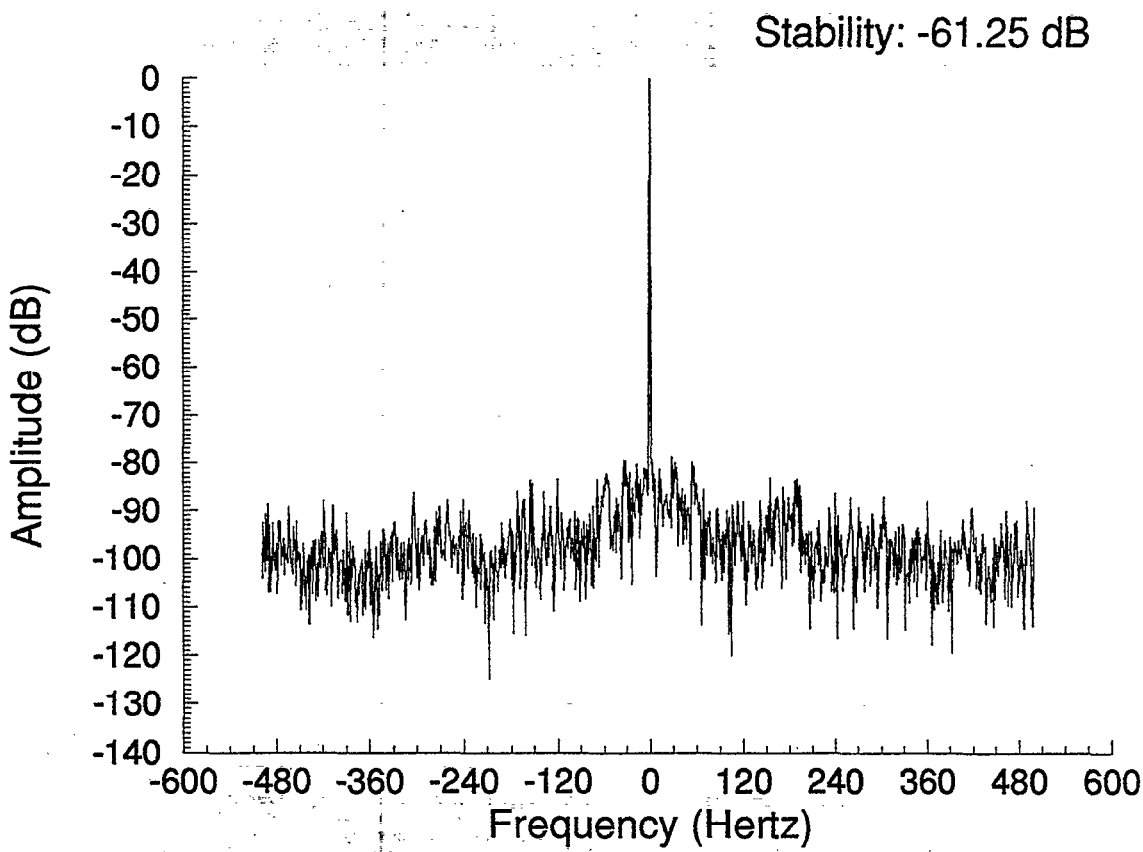

Figure 4b. Field Test: Edited MTS Data (no Doppler).

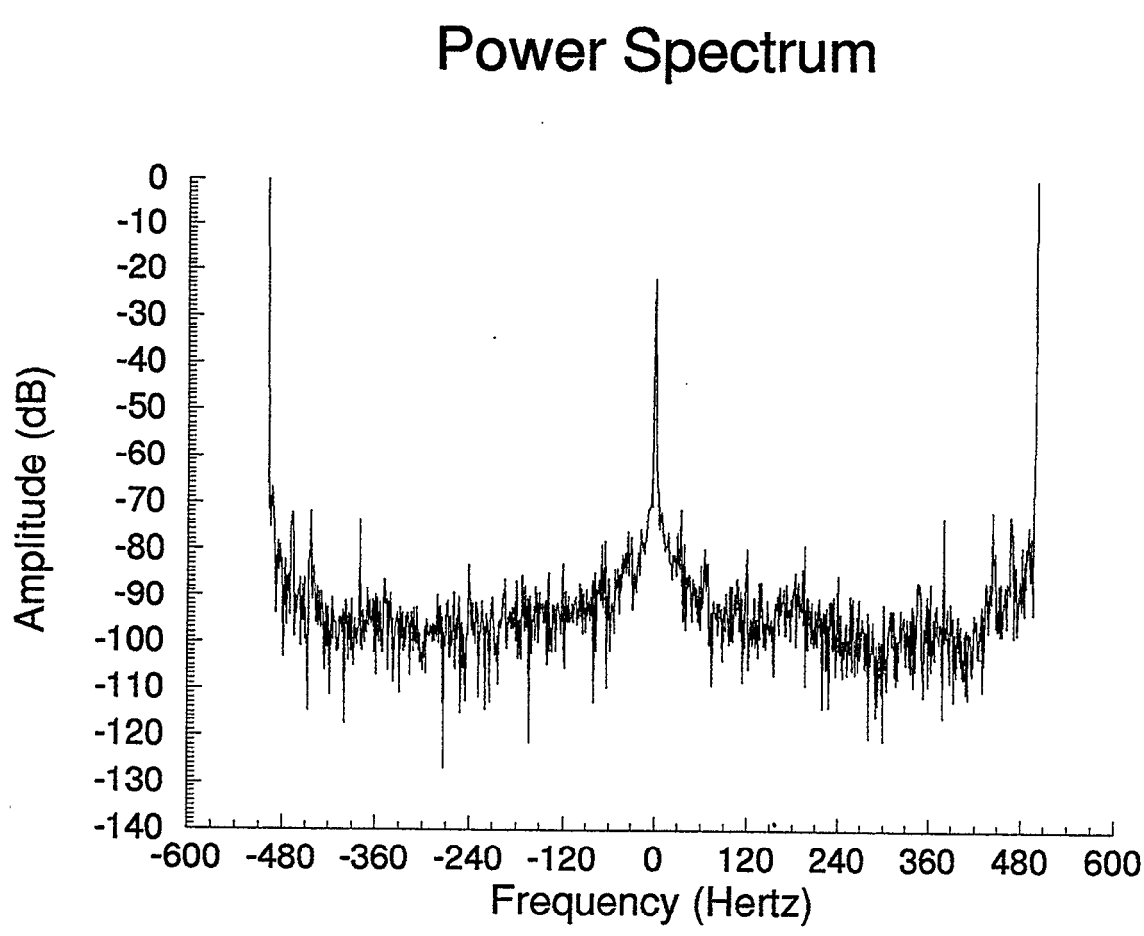

Figure 5a. Field Test: Raw MTS Doppler Data.

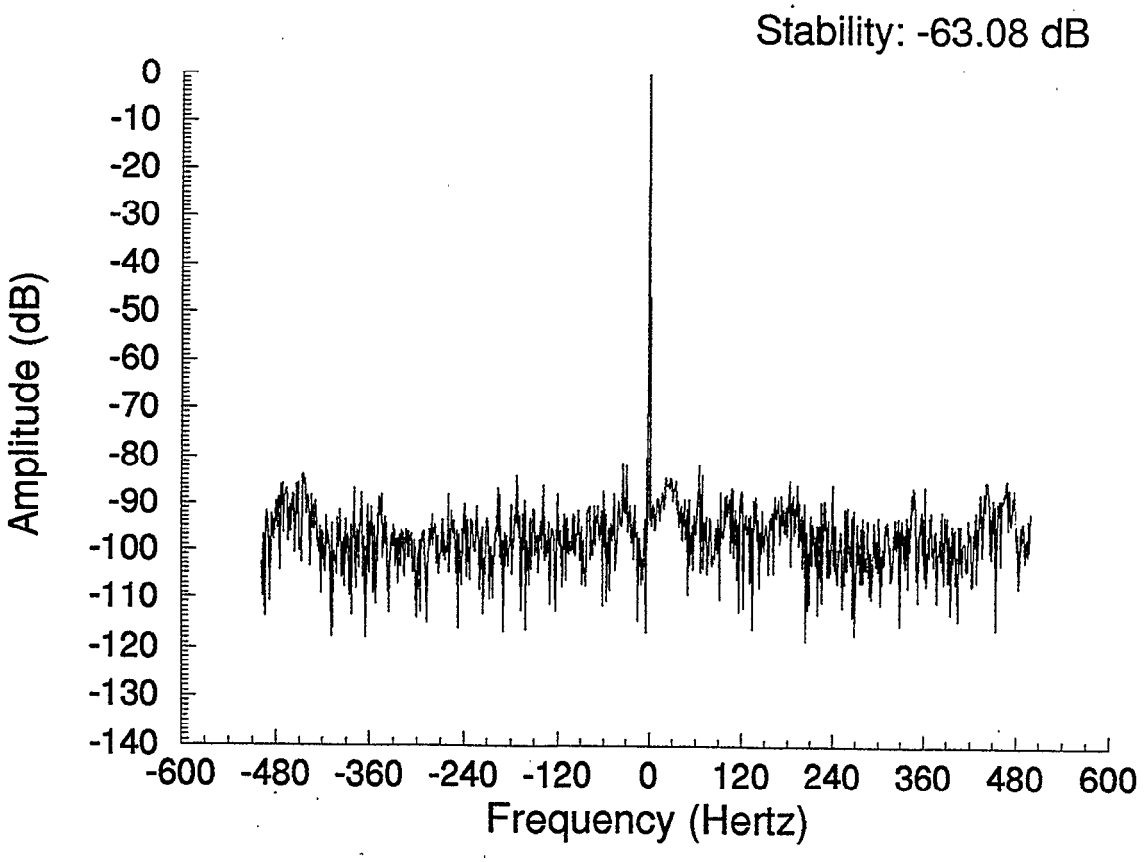

Figure 5b. Field Test: Edited MTS Doppler Data.

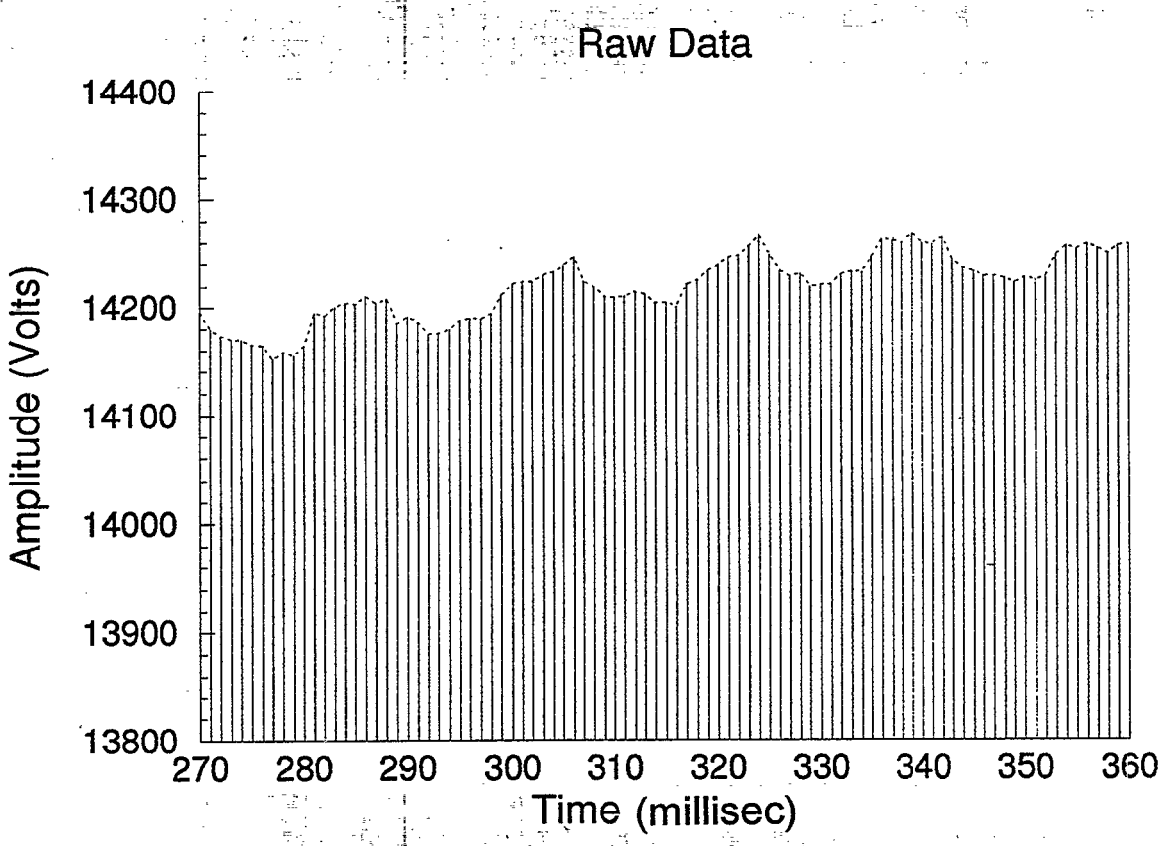

Figure 6a. Amp. vs. Time for Staggered PRF MTS (no Doppler).

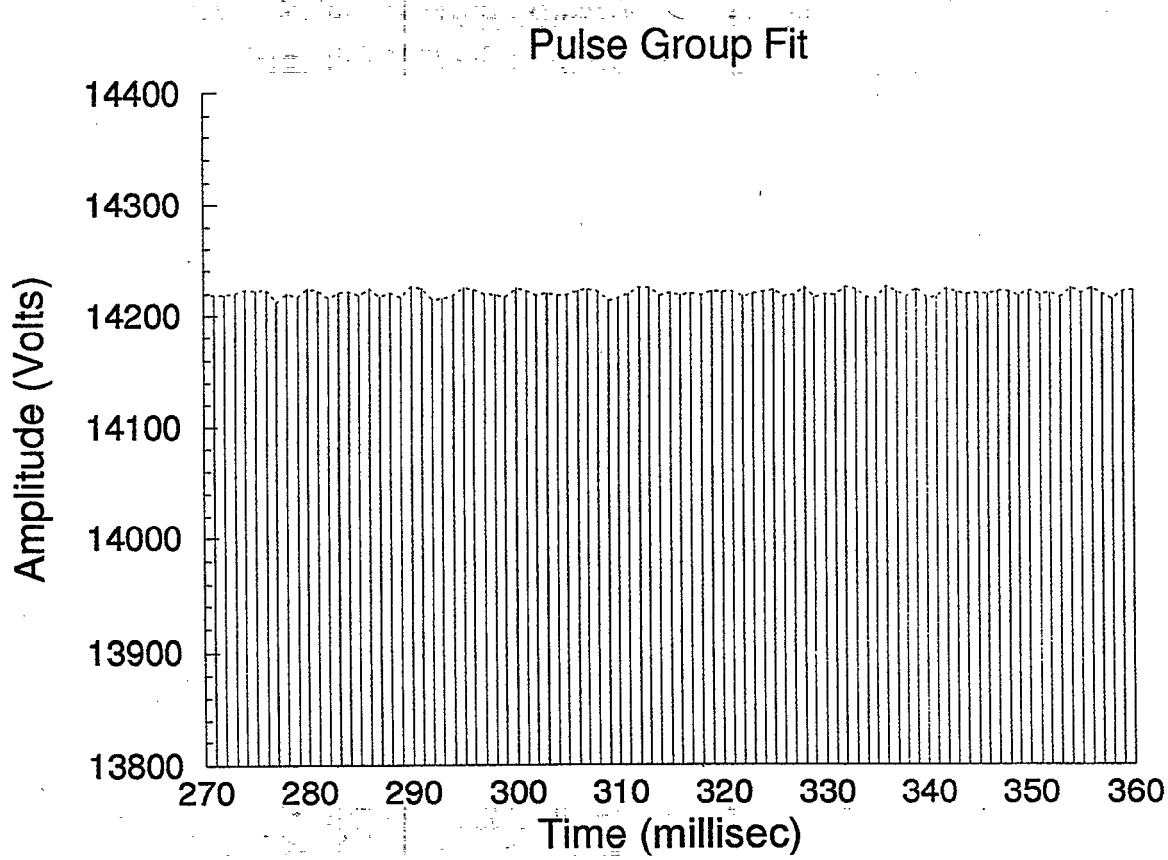

Figure 6b. Amp vs. Time for Staggered PRF MTS (no Doppler).

In all cases, stability was calculated in both the time and frequency domains. Time domain results were obtained by comparing the average (DC) power of the data to its varying (AC) power. Frequency domain results are calculated by comparing the power in the DC line (or 1/2 PRF line when the repeater is used as an MTS) to the sum of the powers in all other frequency bins. The results are expressed as a power ratio in dB.

3.1.1.5 Results

Results for all the field measurements, whether at fixed or staggered PRF's, and whether or not the repeater was operated in doppler mode, were very consistent. Stability measurements for the fixed PRF mode (as indicated in Figure 4) were 61 dB. The average stability for the staggered PRF mode was 62 dB. A plot of the stability estimates for a typical run of staggered pulse groups is shown in Figure 7. Three 1024-point data runs each were taken for fixed and staggered PRFs, with and without the doppler modulator enabled in the repeater.

Local loop tests revealed that the repeater had a stability floor of about 71 dB. This is 9 dB better than the field measurement results, so the repeater did not compromise the stability measurement. It was interesting to note that power-line related spurious (such as seen in Figure 4) were present without the repeater in the loop, so the repeater's power supply was very clean. The radar's power line components are, however, at a very low level.

The pulse stagger data reveal an interesting phenomenon relevant to the application of the Gilfillan transmitter to windshear/microburst detection. The windshear channel uses 27 pulses sampled across a 10-8-10 pulse stagger group. The signal processor interpolates the data to obtain higher resolution doppler spectra across these pulse groups. In Figure 8 we see that for the solid state transmitter, the average phases of each 8 or 10 pulse group changes in a step fashion, that is, the 8 pulse group has an average phase approximately 0.3 degrees different from the 10 pulse group. Unless this effect is compensated in the windshear channel signal processor, the stability of the 27 pulse transform will be affected by the step phase change. If we take this 0.3-degree phase shift to be a typical value, and apply a simple FM sideband calculation [2], then the resultant 27-pulse stability degrades to 52 dB. However, since the pulse group phase change is deterministic and appears to be quite stable, a compensation algorithm similar to that used for the pulse-stagger thermal effects compensation can be applied in the real-time signal processor.

3.1.2 Time Sidelobes

3.1.2.1 Introduction

Because solid-state radar power amplifiers have limited peak output power, they use pulse compression techniques to increase the energy on target to that comparable to a conventional short-pulse high peak power klystron-based transmitter. However, pulse compression results in undesired time (range) sidelobes, and if means are taken to suppress their amplitude at any one doppler, the range sidelobe levels generally increase for other dopplers. As in any matched filter process, time sidelobes extend from the target return to the range equivalent of the uncompressed pulse length in front of the target, to the range equivalent of the uncompressed pulse length behind the target.

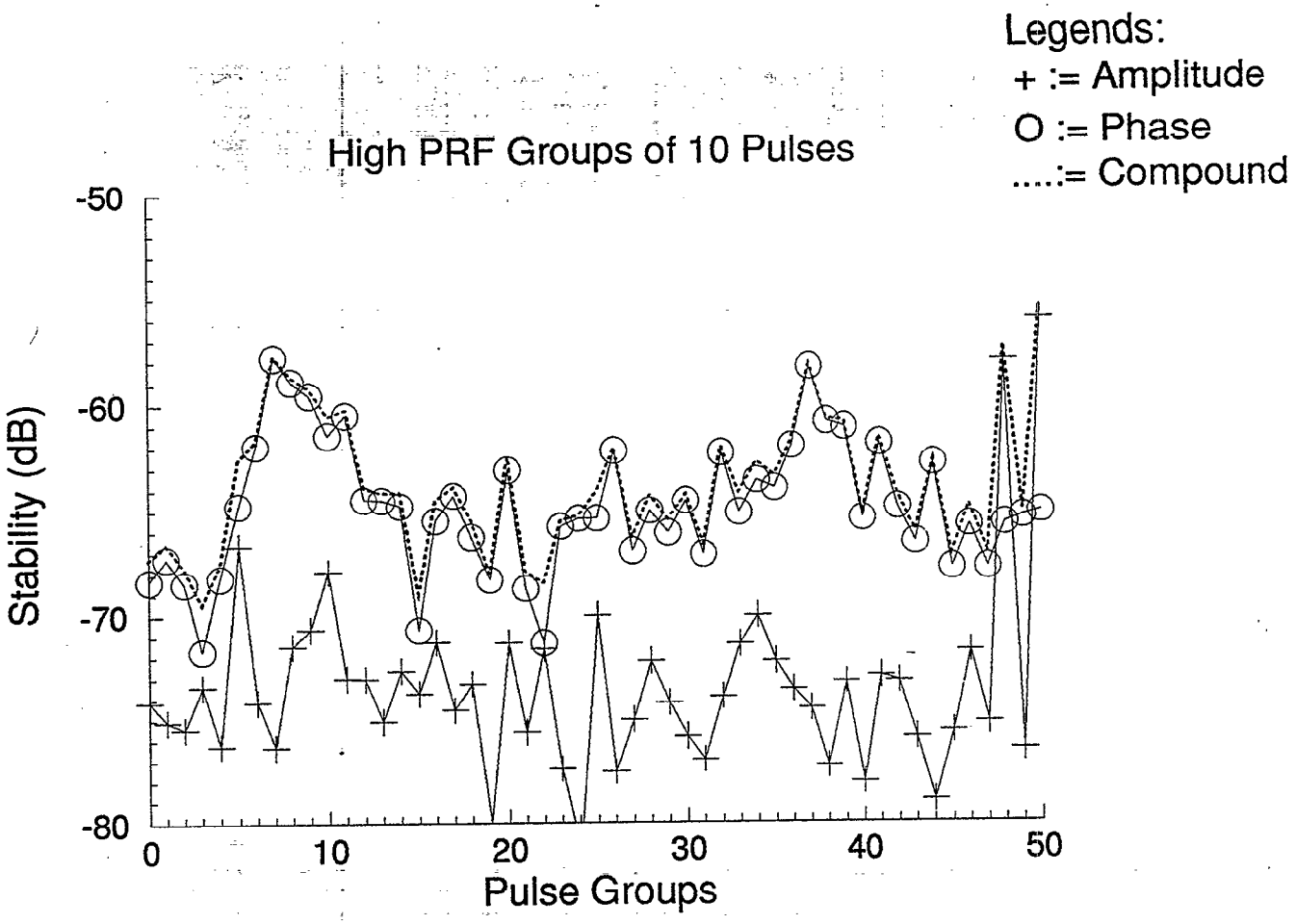

Figure 7a. Stability vs. Pulse Group (no Doppler).

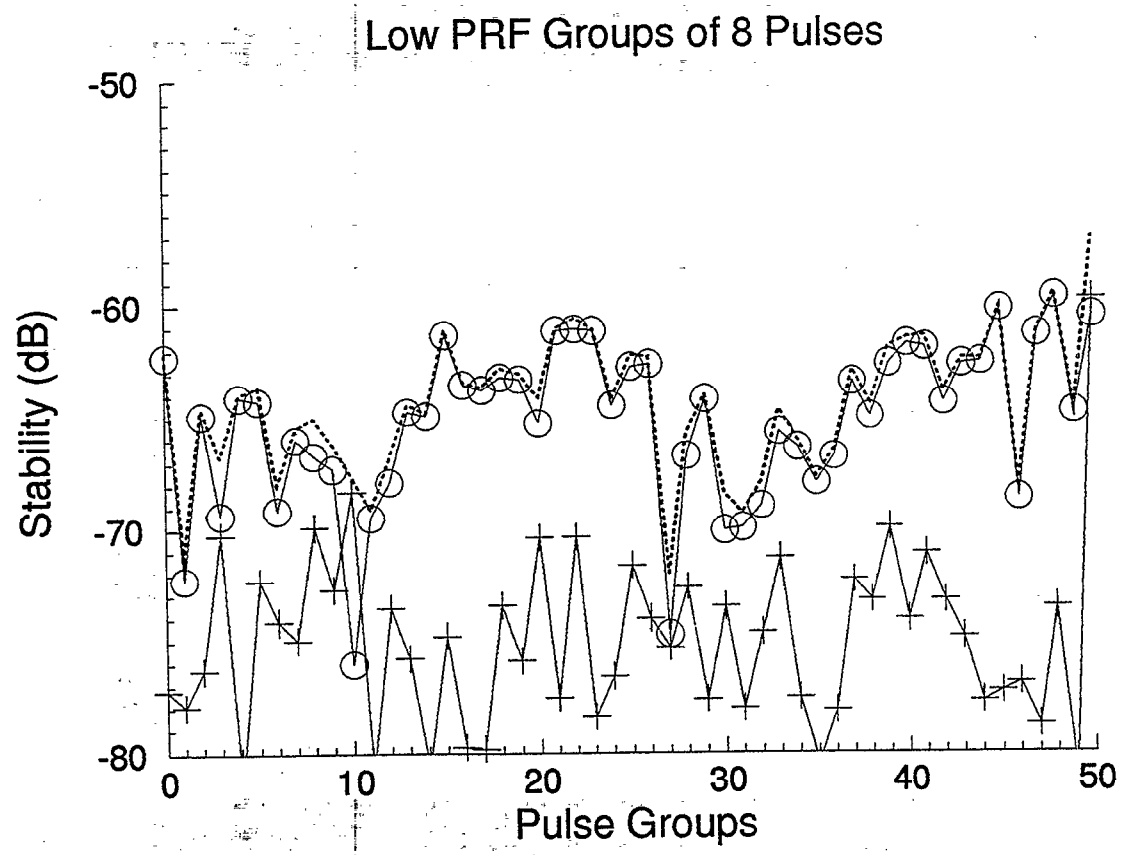

Figure 7b. Stability vs. Pulse Group (no Doppler).

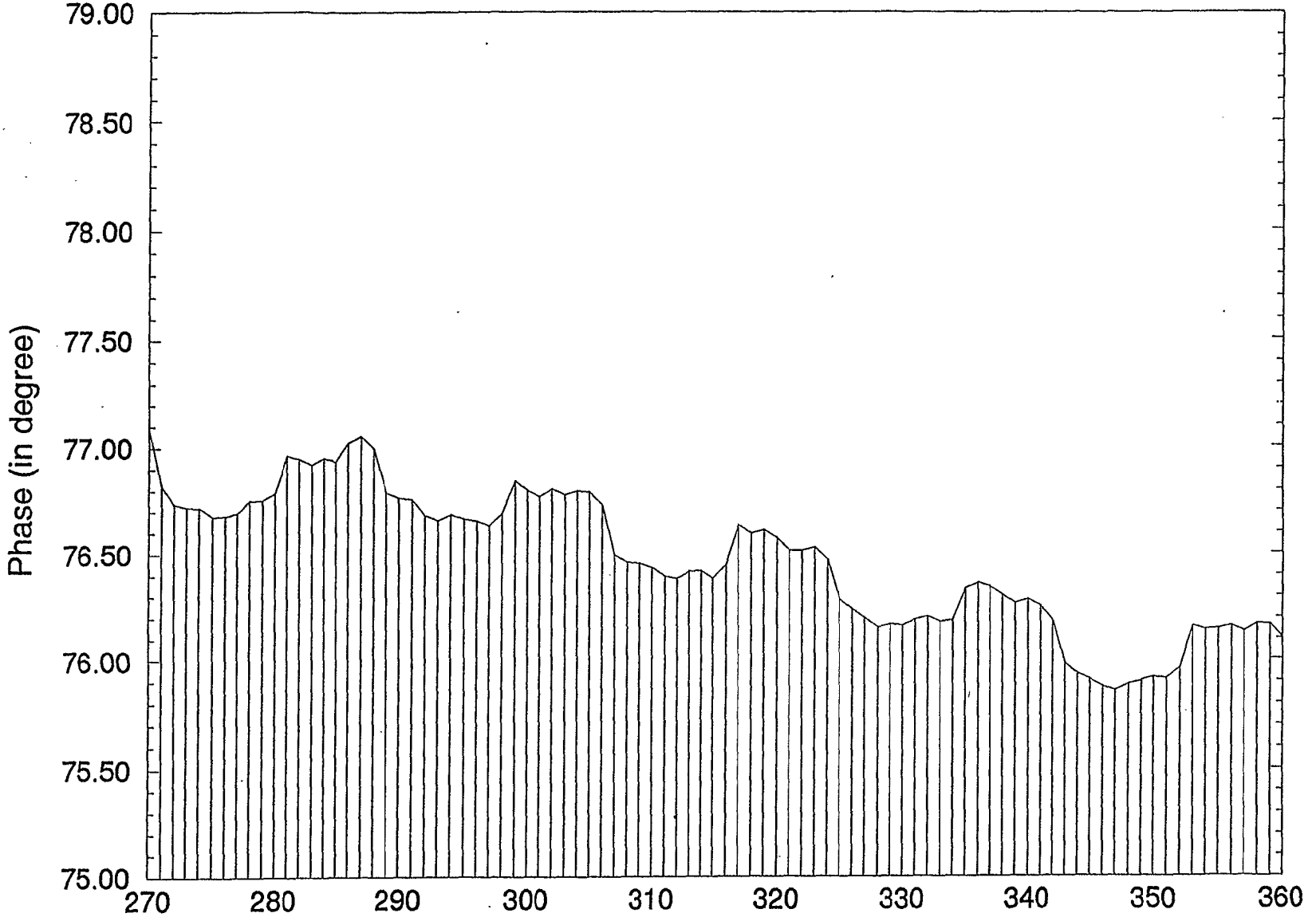

Figure 8. Phase vs. Pulse Group (no Doppler).

The Thomson pulse compression system uses a proprietary nonlinear FM waveform with time sidelobes that remain at very low levels over a wide range of doppler shifts. The uncompressed pulse is 75 microseconds long, so the range sidelobes extend approximately 6 nmi in range and out range from the compressed target return.

3.1.2.2 Measurements

Time sidelobes were measured using loop test methods, that is, by coupling the transmitter/exciter directly back to the receiver through a cable or with various test items interposed. No time sidelobes were observed during target detections (no target signal had sufficient signal-to-clutter level), except when the radar repeater was employed. (As mentioned above, the repeater was designed to provide a near-saturation level signal into the radar. Time sidelobes were at the same level with the fielded radar repeater as were observed during the loop tests.)

Loop tests were conducted with and without the repeater in line, with and without the doppler modulator engaged, with and without the transmitter in the loop, and at varying doppler shifts imposed by the waveform generator in the Thomson exciter. In addition, time sidelobe levels were checked with a Lincoln-designed 100-microsecond delay line in the loop, to see if the levels were range dependent.

A final measurement was to substitute three spare "cold" transmitter power amplifier modules for three randomly chosen "hot" modules operating in the transmitter. The intent was to see if the time sidelobes were degraded by the random substitution of cold spares for operating modules. We also compared the sidelobe levels when the entire transmitter had the operating for several hours to the levels when the transmitter had been operating for about 5 minutes from a cold start.

3.1.2.3 Results

The pulse compression time sidelobes were approximately 55 dB down at all the doppler shifts available in the exciter (and looped repeater), whether or not the 100-microsecond delay line was added to the loop. Figures 9 to 13 show the time sidelobe level as a function of doppler shift; -51 dB worst case peak time sidelobes occurred at a doppler corresponding to a 130-meter/sec target. Note that although the detailed structure of the time sidelobes changes at differing dopplers, the average value changes little at different shifts. There were negligible time sidelobe differences between cold/hot transmitter module swaps or between a transmitter that had been operating for several hours and a transmitter that had been operating for about 5 minutes from a cold start.

Figure 14 illustrates the system time sidelobe performance without the transmitter in the loop, that is, the exciter only was looped into the receiver. No doppler shift was imposed on the exciter signal. Peak sidelobes are 55 dB down, but the average sidelobe levels are nearly 70 dB down. Compared to Figures 9 to 13, which are loop tests that include the Gilfillan power amplifier, we note that the amplifier's nonlinear phase runout and amplitude droop contribute significantly to the average sidelobe level, even though the pulse compressor uses a transmitter compensation algorithm. The comparison underscores the sensitivity of these very low time sidelobe levels to minor mismatches in transmitter phase runout and amplitude droop compensation algorithm.

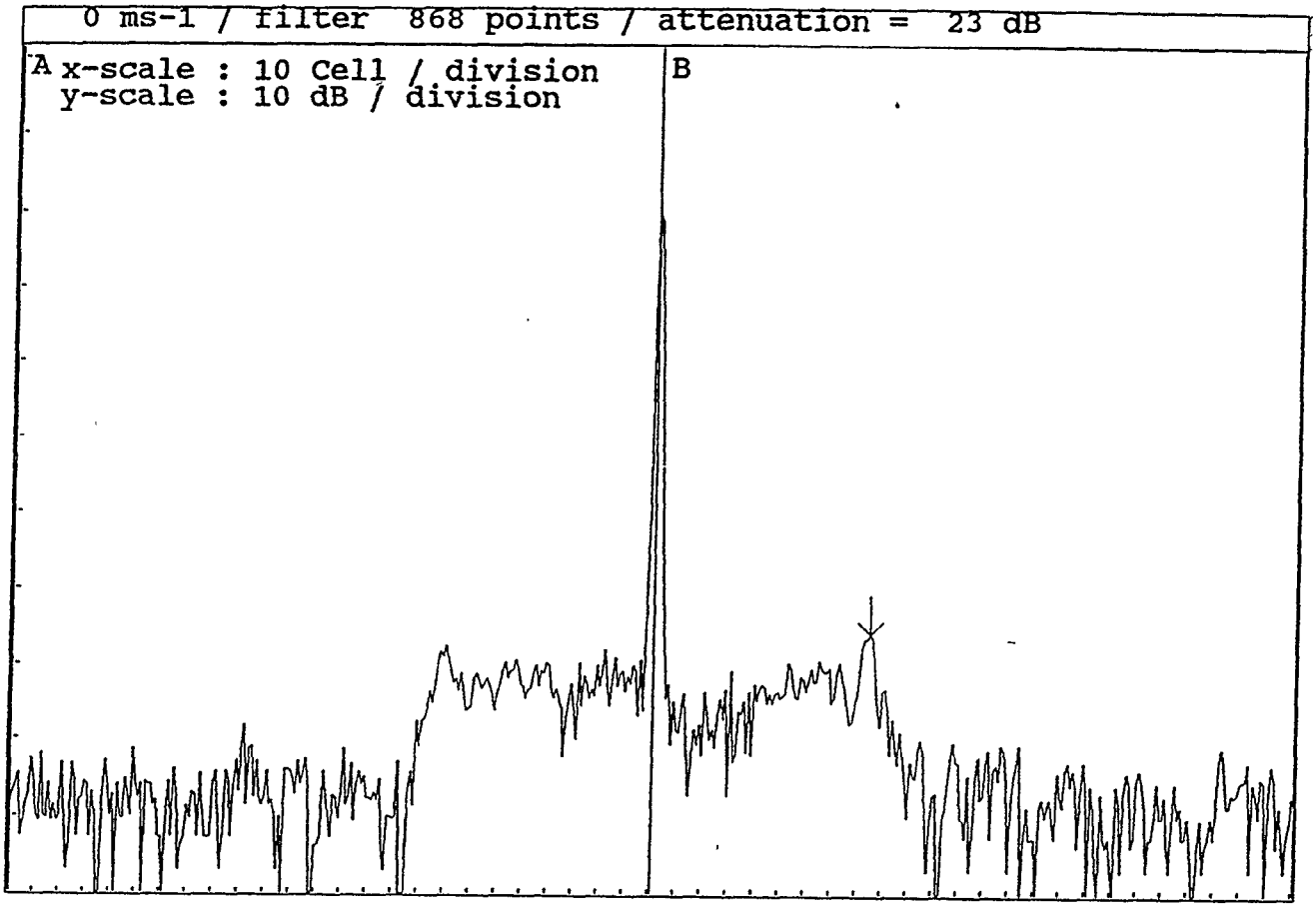

Figure 9. Radar Time Sidelobes, 0 m/sec Doppler.

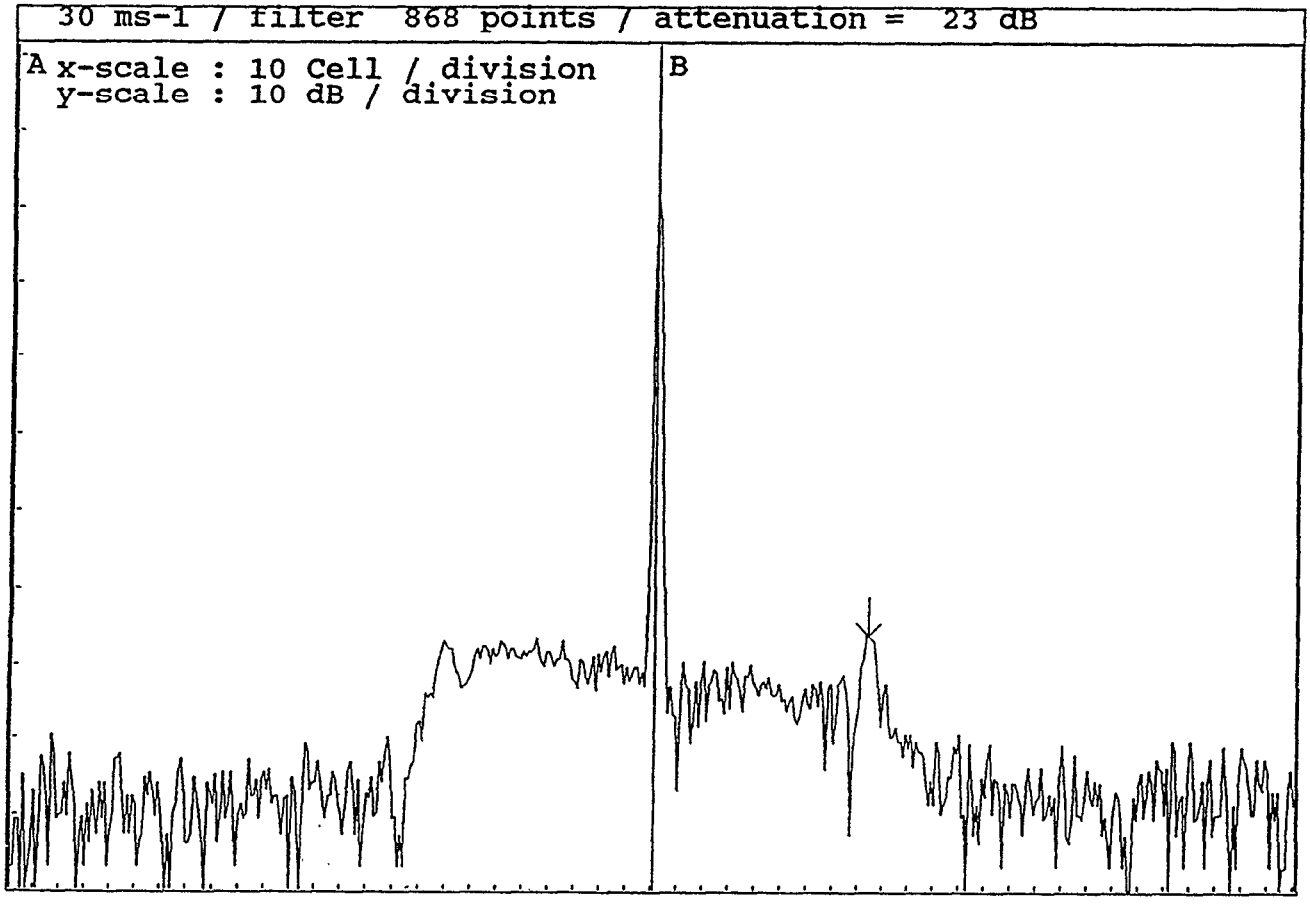

Figure 10. Radar Time Sidelobes, 30 m/sec Doppler.

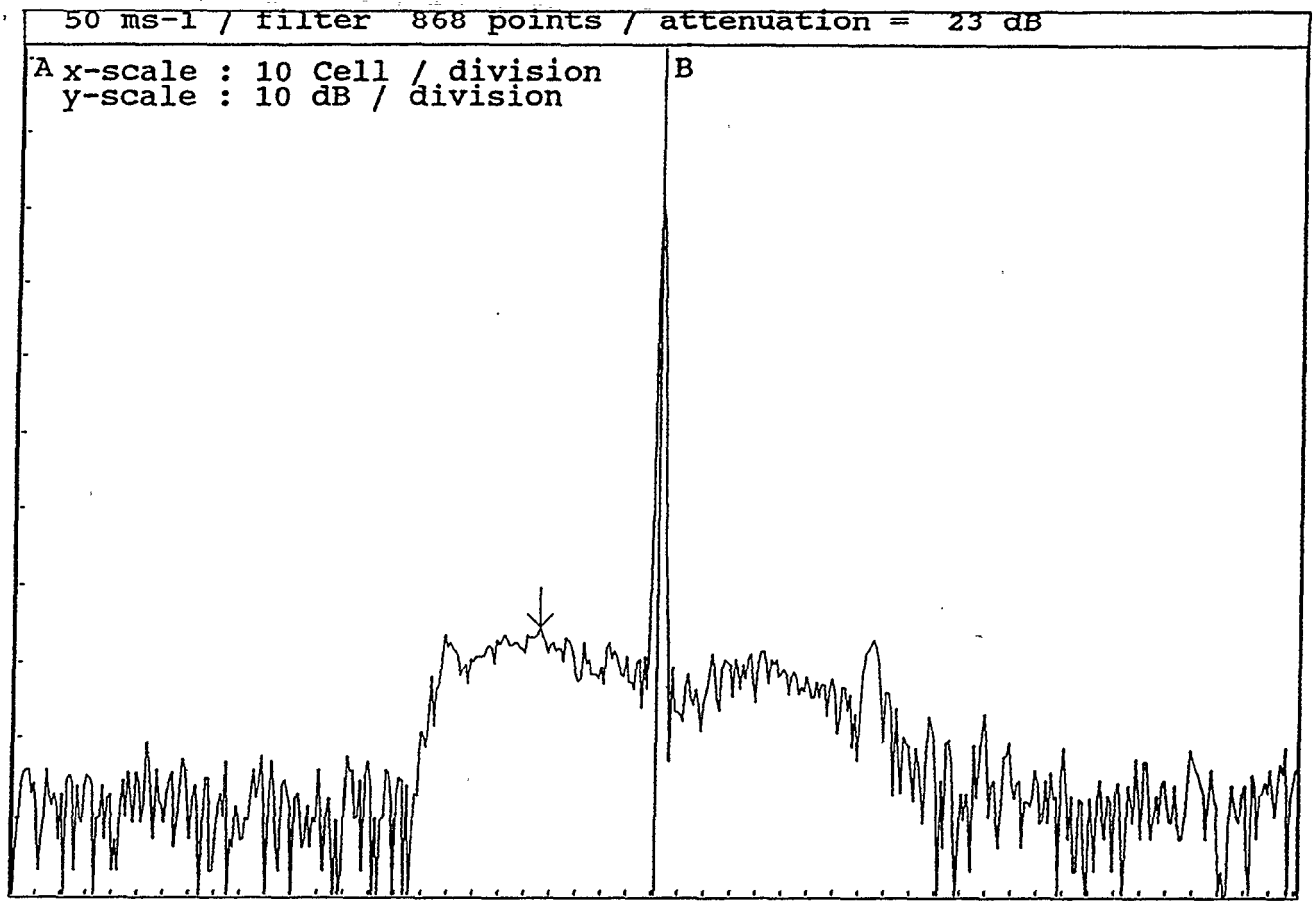

Figure 11. Radar Time Sidelobes, 50 m/sec Doppler.

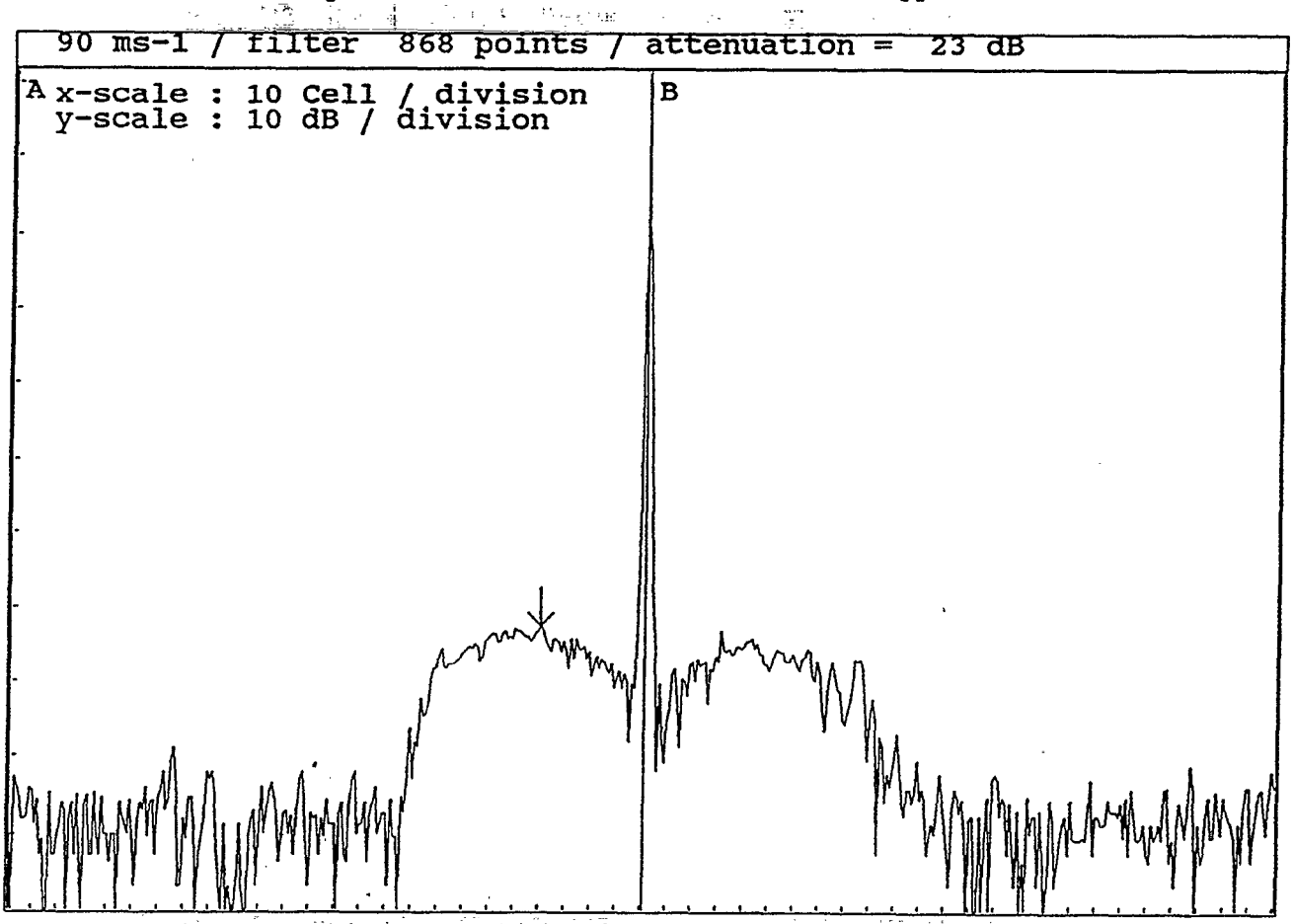

Figure 12. Radar Time Sidelobes, 90 m/sec Doppler.

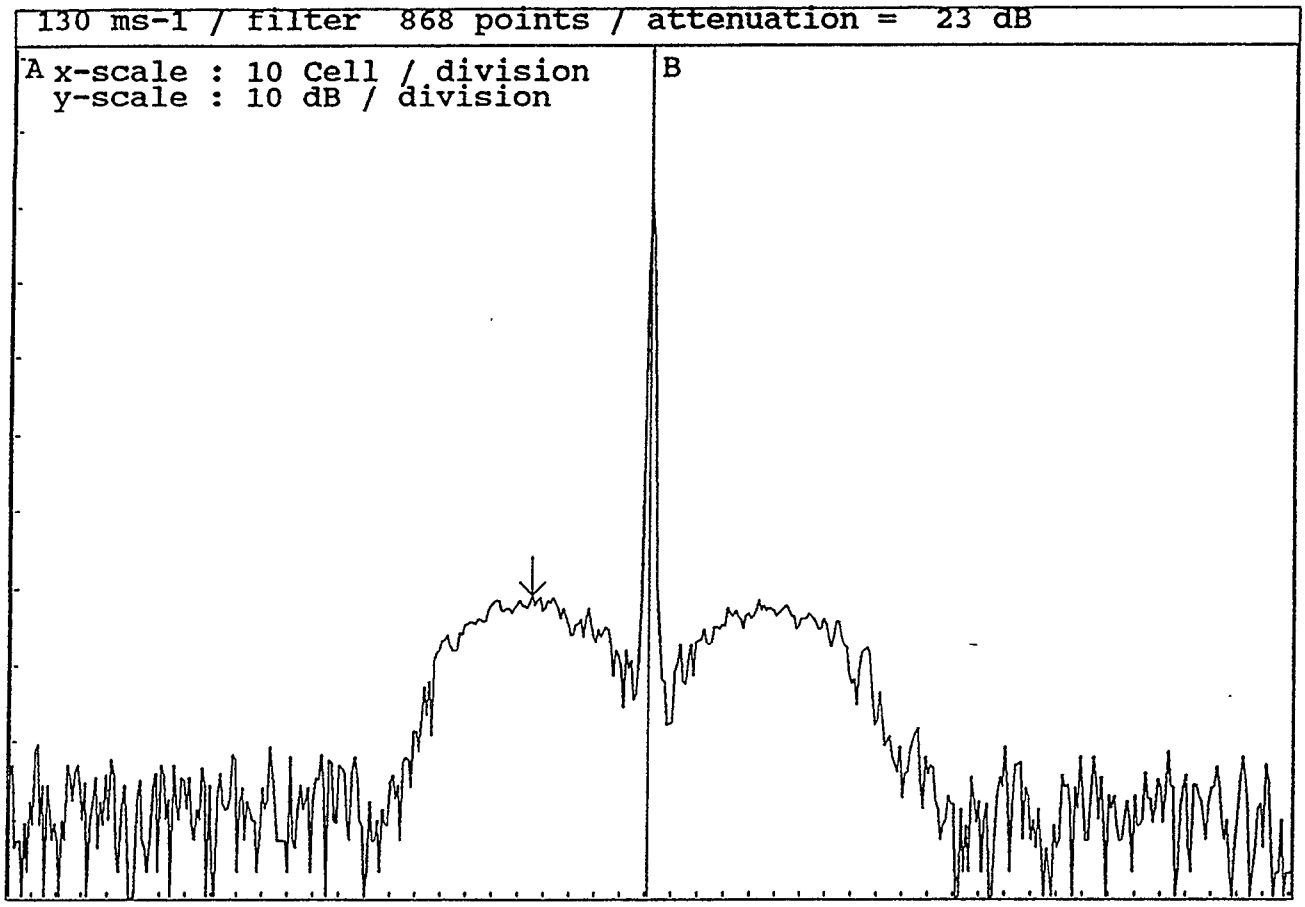

Figure 13. Radar Time Sidelobes, 130 m/sec Doppler.

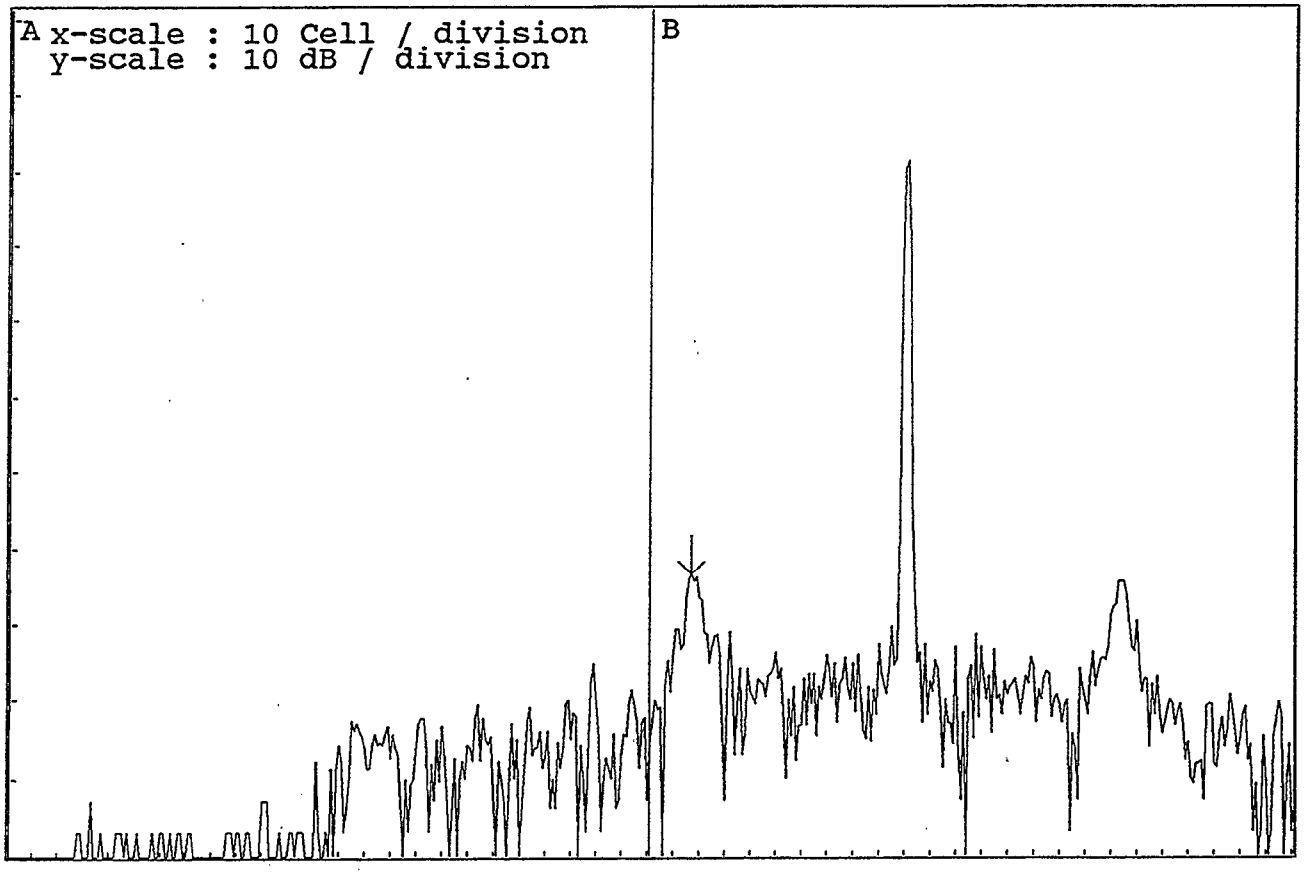

Figure 14. Radar Time Sidelobes, Exciter only, No Doppler.

Although the peak sidelobes remain low, the increased average time sidelobes from unwanted transmitter effects and from doppler shifts will correspondingly increase the integrated time sidelobe level. The integrated time sidelobe level is simply the ratio of the energy in the main target response to the total energy in the time sidelobes. Low integrated time sidelobes are important to minimize range smearing near extended targets with high reflectivity gradients and complex doppler signatures, like thunderstorms. The integrated time sidelobes for the Thomson/Gilfillan radar range from about -43 to -35 dB, depending on the transmitter compensation and doppler. These levels may be adequate, but no demonstration data were taken to confirm weather detection performance. Additional field data and detailed simulations would be required to properly address this issue.

3.1.2.4 Short Pulse Interference

During the demonstration at the FAATC, interference from the nearby WSR-57 weather radar was often observed on test equipment connected to the solid state radar receiver. The WSR-57 is a 35-year old magnetron-based radar, operating at S-band (the same frequency range as the ASR-9). It is a high peak-power, short pulse radar.

Figure 15 shows a typical range profile (amplitude vs. range) along a single radial taken with the Gilfillan/Thomson radar. This range profile covers a range of 16 nmi, with the short pulse/long pulse transition occurring at 7.8 nmi, about half way across the plot. The range profile of the very next PRI, taken along essentially the same radial, is shown in Figure 16. Note that the amplitude of the "clutter" from the short pulse/long pulse transition to about 6 nmi outrange has increased by about 20 dB. The range profile of the next PRI appears again like Figure 15.

The briefly increased signal amplitude over that 6 nmi range extent is due to the effects of short pulse interference from the WSR-57. The interfering short pulse (approximately 1 microsecond long) acts as an impulse-like excitation for the 75-microsecond pulse compression filter. The filter rings for 75 microseconds (6 nmi in range), just as an analog pulse expander forms long pulses from an impulse excitation. It appears that considerable amplitude weighting is used in the Thomson pulse compressor, because of the rounded impulse response observed in this range profile (amplitude weighting is used to make a nonlinear FM waveform less sensitive to doppler shifts at the expense of increased mismatch loss).

The extended range interference from short-pulse emitters exhibited by the Thomson equipment is an inherent characteristic of pulse compression receivers. A conventional short-pulse radar receiver (not using pulse compression) would have been affected over 1 range gate, not 75 range gates as in this particular pulse compression scheme. However, a non-pulse compression receiver experiences an interference level 75 times greater than in the pulse compression system; in effect, the pulse compressor spreads the energy over more range bins but at 1/75th the level. Short pulse interference to pulse compression radars is a potentially serious concern, since many dozens of range cells and all doppler filters are affected. The interference will degrade or render ineffective the radar's dynamic thresholding and doppler estimates made on real targets present in the affected range cells. In addition, short pulse interference can be present at many azimuths, depending on the antenna sidelobe performance of the two radars, the spectral purity of the interfering radar, and the selectivity of the pulse compression radar receiver. A modern short pulse ATC radar such as the ASR-9 has a short pulse interference detection and limiting scheme which will not work properly in a pulse compression receiver. Short pulse interference to pulse compression receivers is not an insoluble problem, but it must be addressed in the radar receiver and processor design if pulse compression is to be successfully fielded in ATC radar applications.

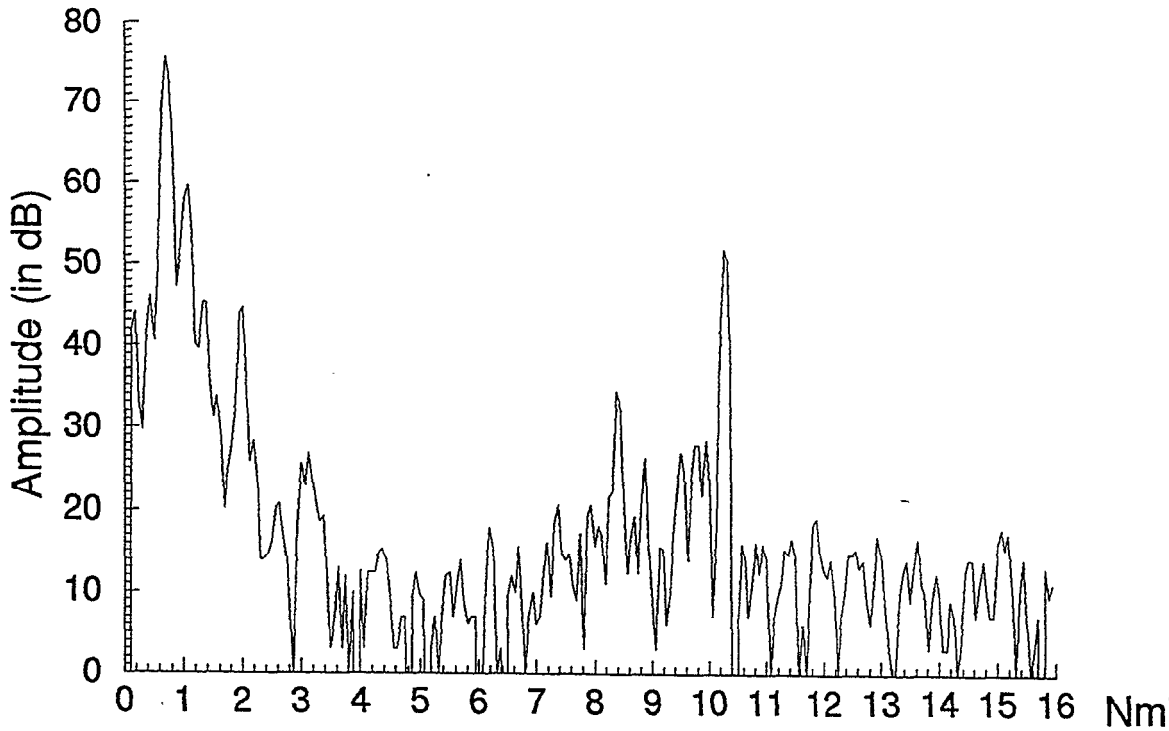

Figure 15. Range Profile - No Interference.

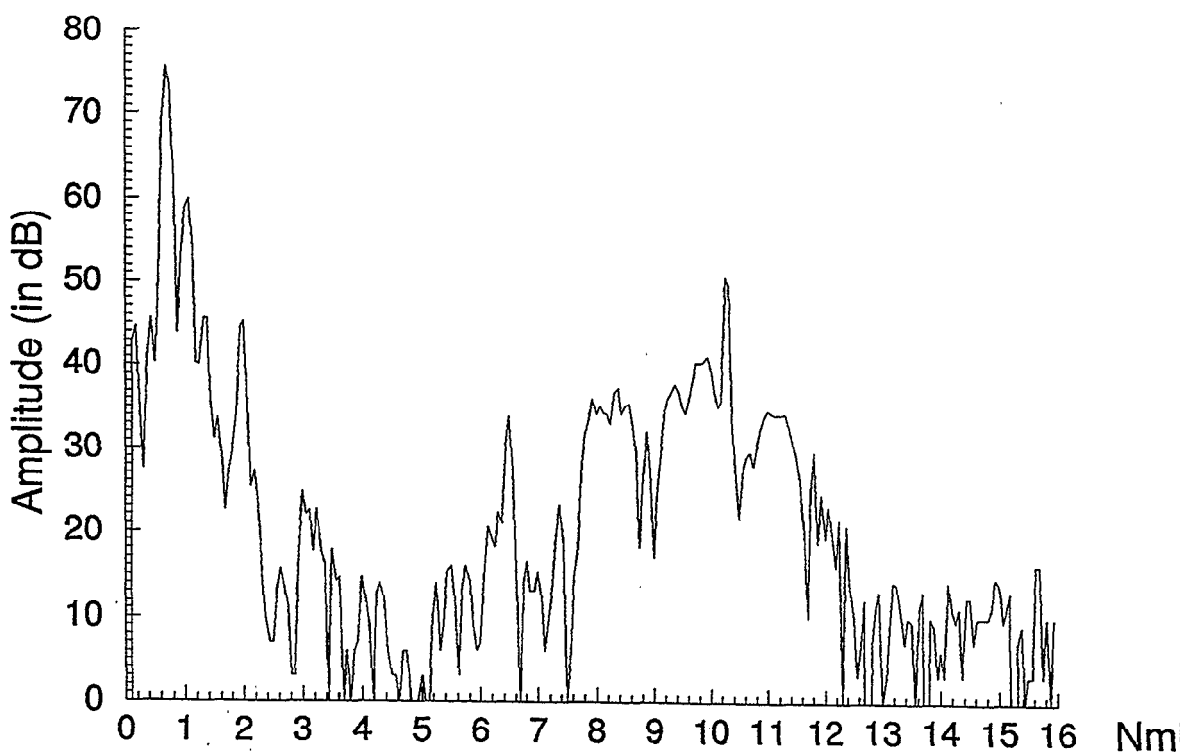

Figure 16. Range Profile with Short Pulse Interference.

3.1.3 Detection Performance

As indicated above, the limited peak power of the Gilfillan solid state power amplifier requires that a long pulse be used to obtain sufficient energy on target at long ranges. This pulse is 75 microseconds long, which masks close-in targets up to about 6 nmi from the radar. A short (1 microsecond long) pulse is also transmitted after the long pulse, and at a different frequency, to fill in the 6 nmi range swath blanked during long pulse transmission.

Enough energy is in the long pulse to yield target detection capabilities identical or slightly better than that of an ASR-9. A simple calculation shows that if the short pulse/long pulse transition is set to occur at 7 or 8 nmi, the short pulse energy is also sufficient to ensure ASR-9 like target detection for the first 7 or 8 nmi.

The solid-state demonstration radar fed I & Q data into the ASR-9 MTD processor. Two limitations arise because of the Thomson/Gilfillan decision to use the ASR-9 MTD: (1) The 18-bit I & Q data from the Thomson receiver was truncated to 12 bits to accommodate the ASR-9; and (2) the ASR-9 MTD processor was not designed for dual pulsewidth waveforms. The latter limitation means that ASR-9 range-averaging CFAR will be biased by the 19-dB energy discontinuity in the vicinity of the short pulse/long pulse transition. This effect, which will tend to set the CFAR threshold too high for the outer range of the short pulse, results in biased target detection statistics as reported at the ASR-9 MTD output.

Limited data were collected to investigate how a MTD processor optimized for dual pulse waveforms might report unbiased target detection. Data were taken on a single flight of a small aircraft at a 4500-foot altitude, flying inbound along a radar radial and crossing over the long pulse/short pulse transition. The transition occurred at 7.8 nmi. For the short pulse, the radar received on the high beam for the first 3 nmi; for the long pulse, the radar received on the high beam from 7.8 to 9 nmi, then from the low beam. STC was applied to the high beam only with a $1/R^3$ characteristic, up to 3 nmi from the radar.

The data were processed by performing a discrete Fourier transform on each of the 8 and 10 pulse complex data samples produced by the Thomson pulse compressor. The processed data are shown in Figures 17 to 22. Each figure plots the doppler filter amplitudes, normalized to the largest return, for the target range gate when the target is present (solid line) and when the target is absent (dotted line). Target absent data are taken from a scan when the aircraft is in another range cell. The target crosses the short/long pulse transition between scans 4 and 5.

Note that in every figure the fourth pulse group shows very little evidence of target presence; this is because the Thomson demonstration recorder could not be set up to center the aircraft radial in the recording wedge. The aircraft is just within the beam for the first three PRI's, and by the fourth PRI, the antenna has scanned away.

Examining the first three pulse groups (an 8/10/8 staggered PRF sequence when the aircraft is in the beam) for several scans as the aircraft proceeds inbound yields:

Scan Number	Range (nmi)	Peak SIR Pulse Grp#1	Peak SIR Pulse Grp#2	Peak SIR Pulse Grp#3
1	9.75	62 dB	62 dB	55+ dB
3	8.56	48 dB	50 dB	31 dB
4	7.93	46 dB	45 dB	27 dB
5	7.38	27 dB	25 dB	7 dB
6	6.75	35 dB	33 dB	13 dB
8	5.50	51 dB	47 dB	23 dB

where the Peak signal to interference ratio (SIR) denotes the signal to interference ratio measured in the target's doppler bin with the target present and absent. The target crosses the short/long pulse transition between scans 4 and 5.

Two observations can be made about this limited data set: (1) Target energy drops by 19 to 20 dB when the aircraft crosses the short/long pulse transition, precisely as would be predicted from the pulse energy difference and the slight range difference, (2) When the target is plainly in the beam (that is, for pulse groups 1 and 2), signal to interference levels for the outer range of the short pulse region (scan 5) yield adequate detection performance. The 25 dB or greater SIR shown will yield a greater than 0.95 probability of detection and a 10^{-12} probability of false alarm against a Swerling I target.

This single data set, with its low altitude target appearing at the edge of the recording wedge, does not address other issues related to target detection with dual pulse lengths. These issues include optimization of the radar's STC, the high/low beam switchover points, and the MTD processor's limited dynamic range and CFAR. The data demonstrate that the solid state radar energy is sufficient for adequate target detection at the outer range of the short pulse waveform, and that the design of a CFAR optimized for dual pulse operation should begin by taking into account the fundamental energy differences between the two pulsewidths.

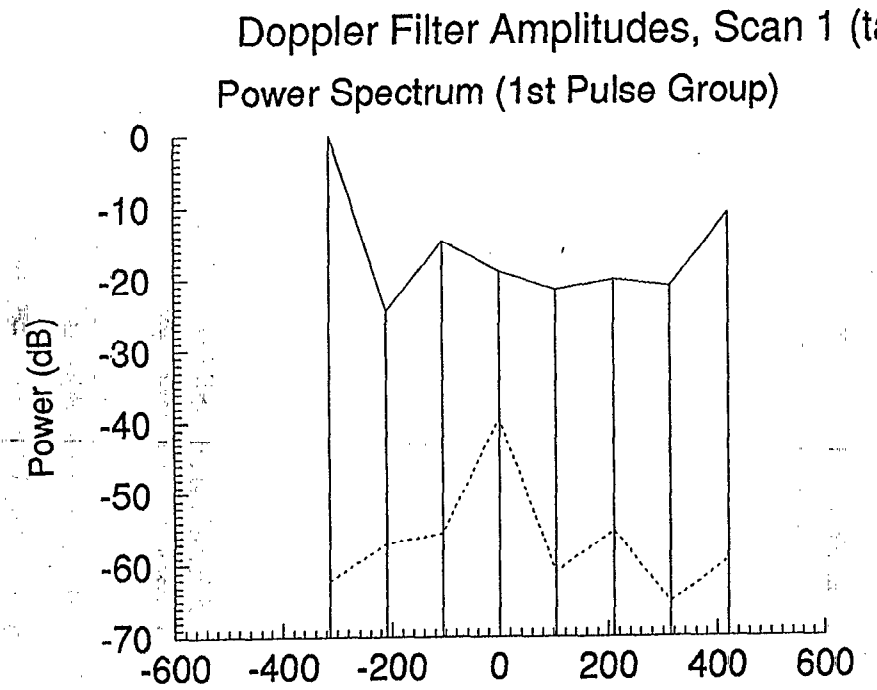

Figure 17a. Doppler Shift in Hertz (8 pulses).

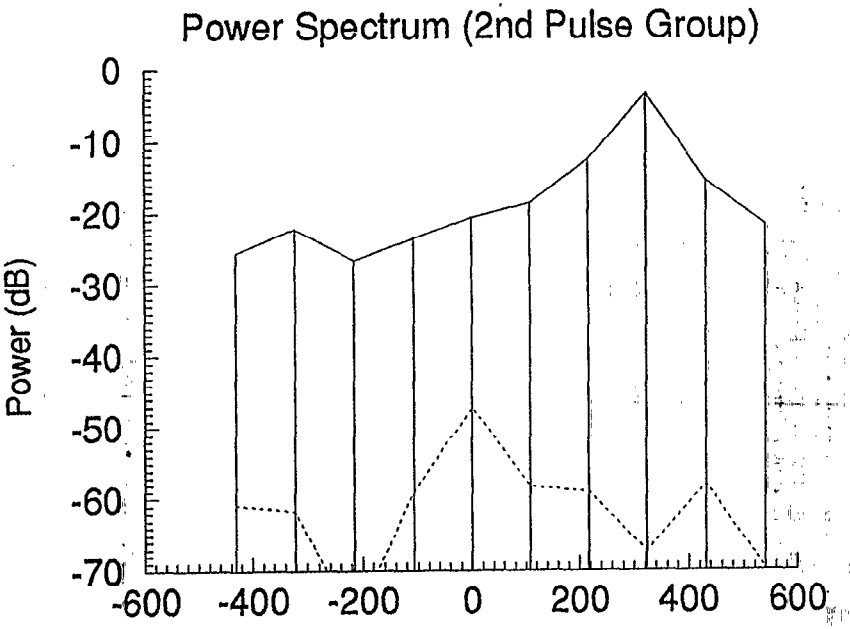

Figure 17b. Doppler Shift in Hertz (10 pulses).

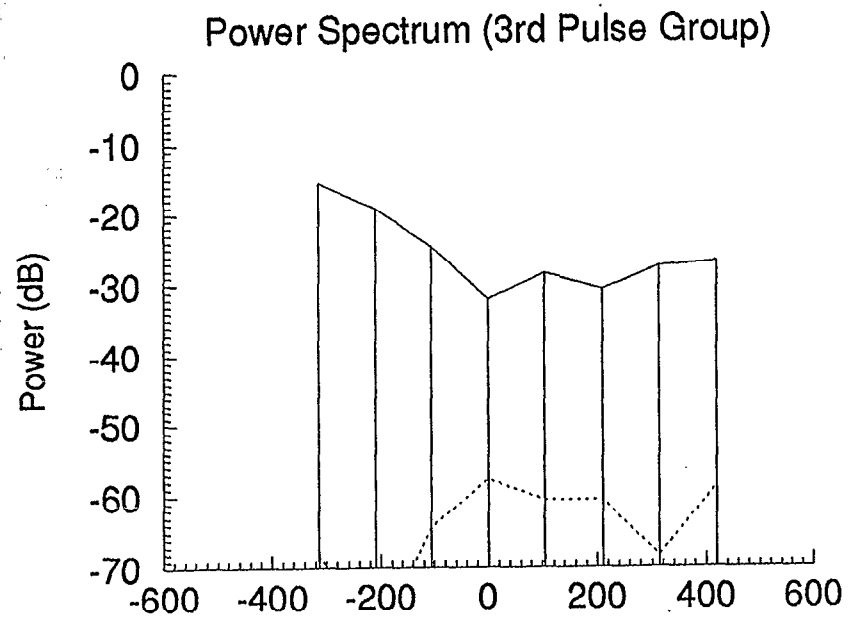

Figure 17c. Doppler Shift in Hertz (8 pulses).

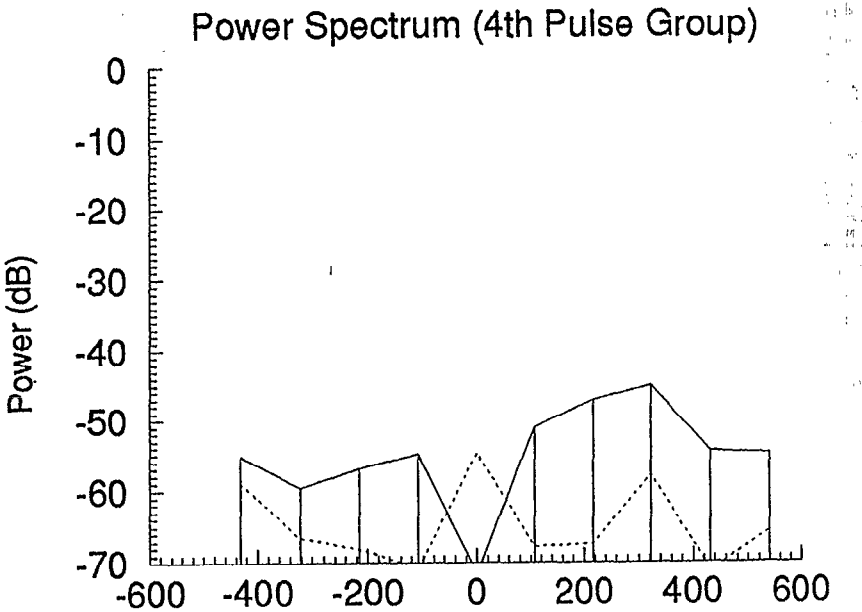

Figure 17d. Doppler Shift in Hertz (10 pulses).

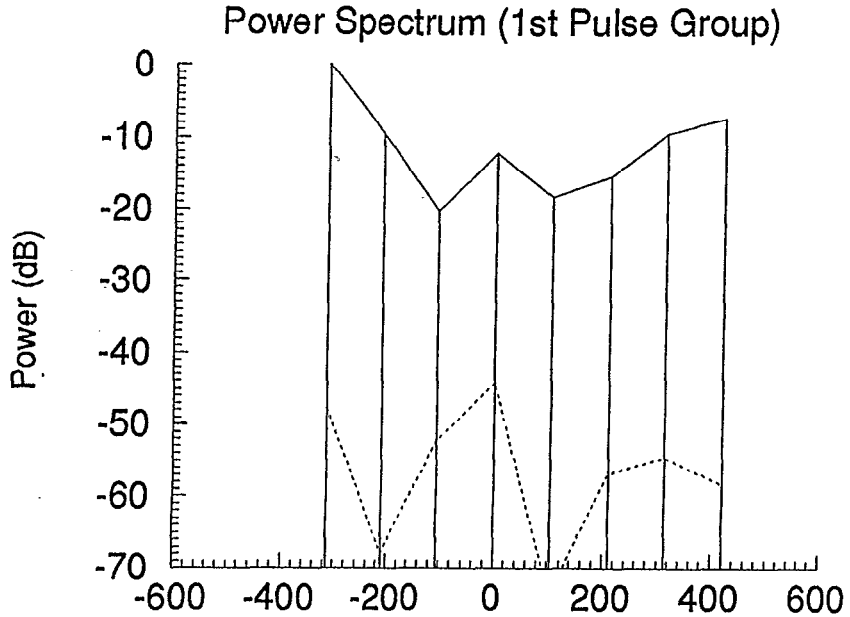

Figure 18a. Doppler Shift in Hertz (8 pulses).

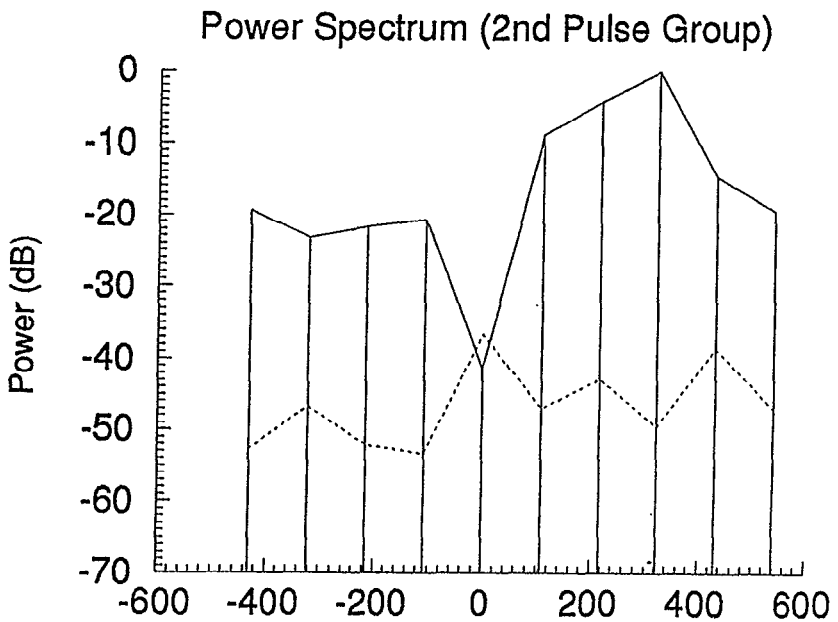

Figure 18b. Doppler Shift in Hertz (10 pulses).

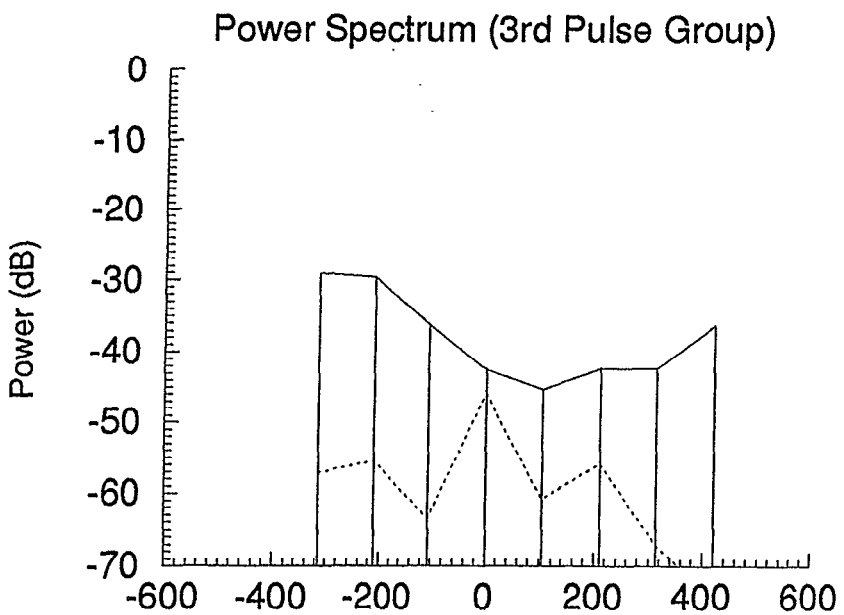

Figure 18c. Doppler Shift in Hertz (8 pulses).

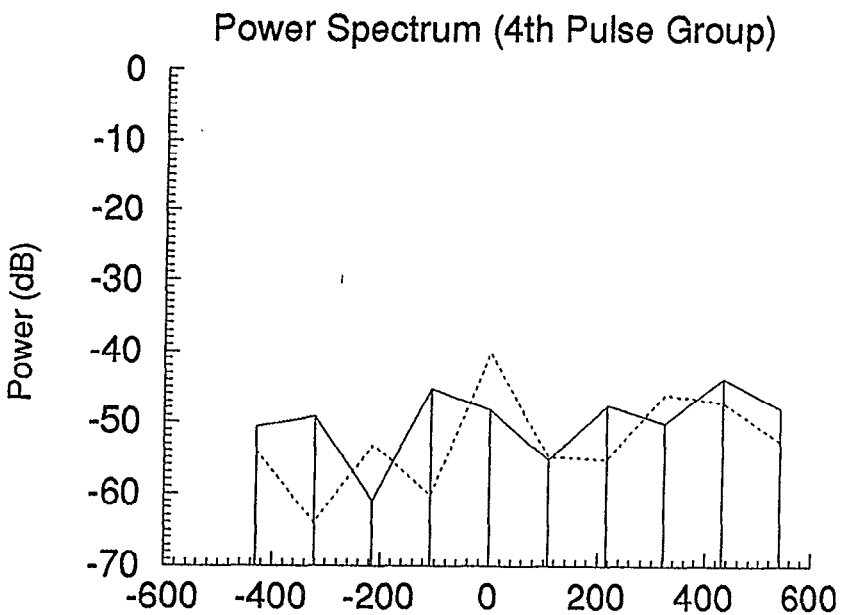

Figure 18d. Doppler Shift in Hertz (10 pulses).

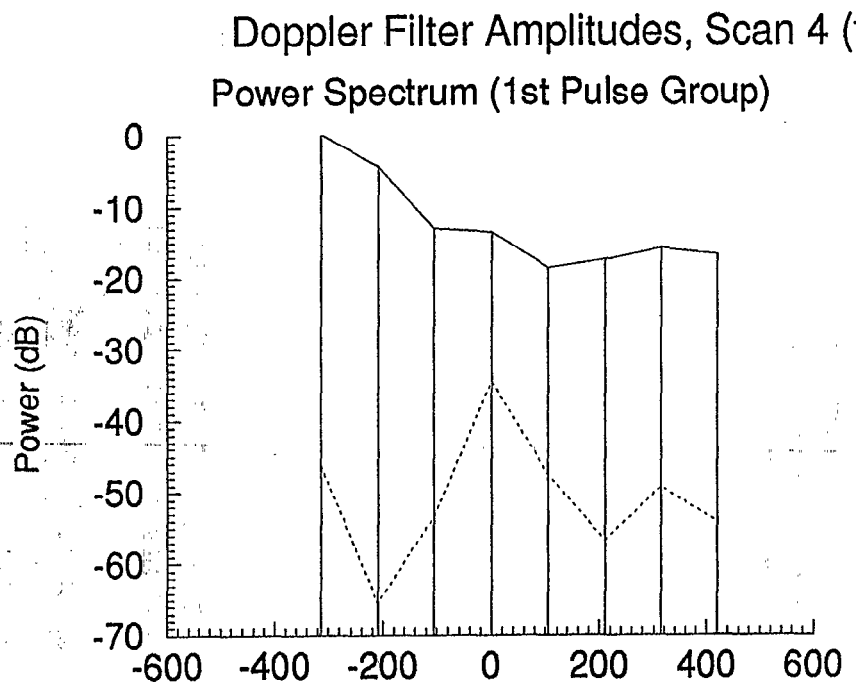

Figure 19a. Doppler Shift in Hertz (8 pulses).

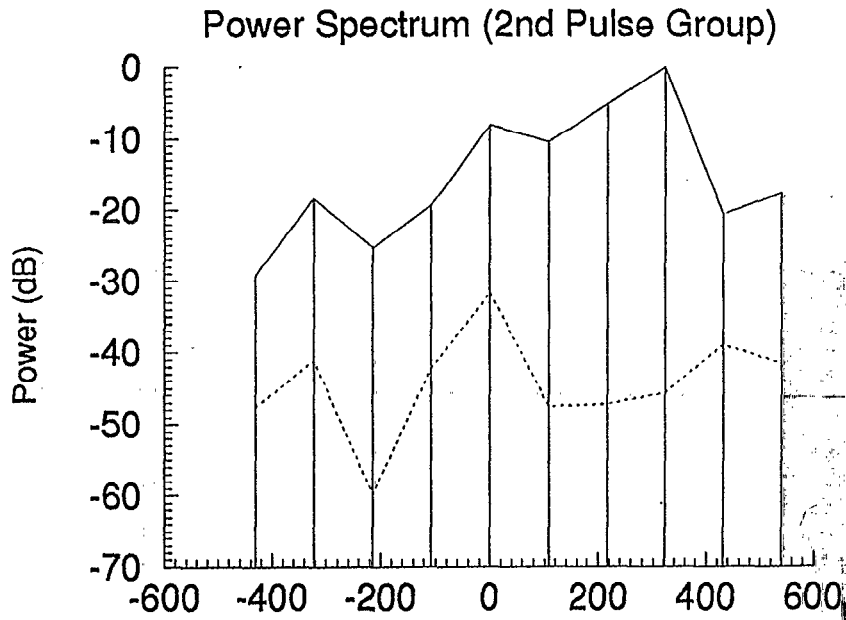

Figure 19b. Doppler Shift in Hertz (10 pulses).

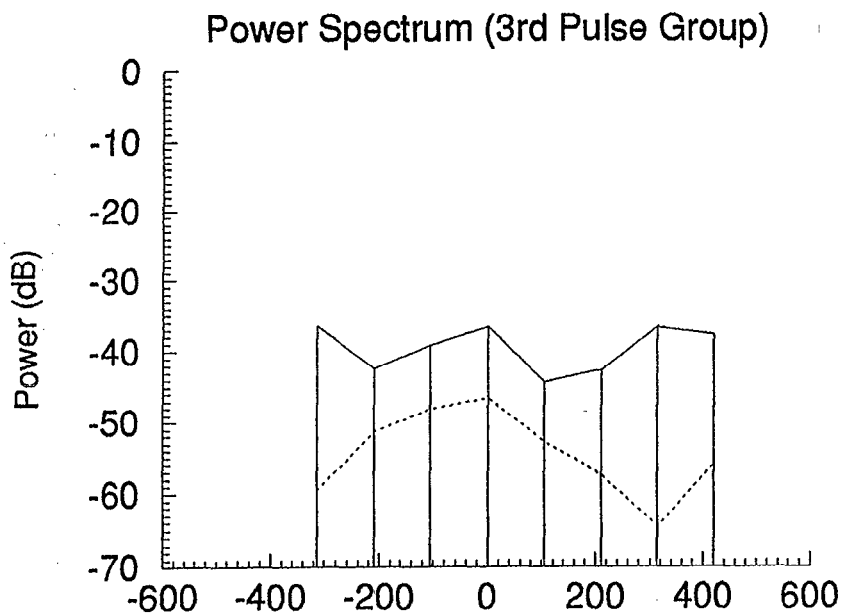

Figure 19c. Doppler Shift in Hertz (8 pulses).

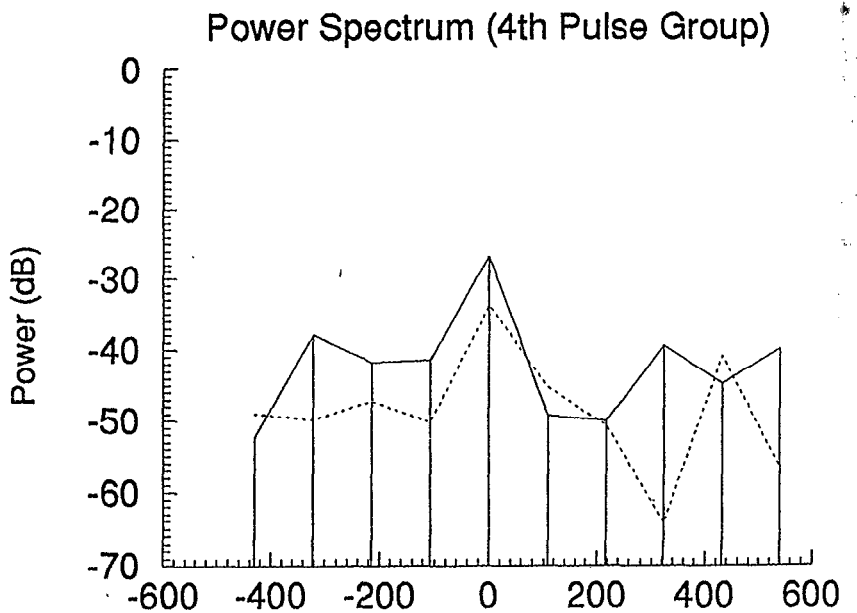

Figure 19d. Doppler Shift in Hertz (10 pulses).

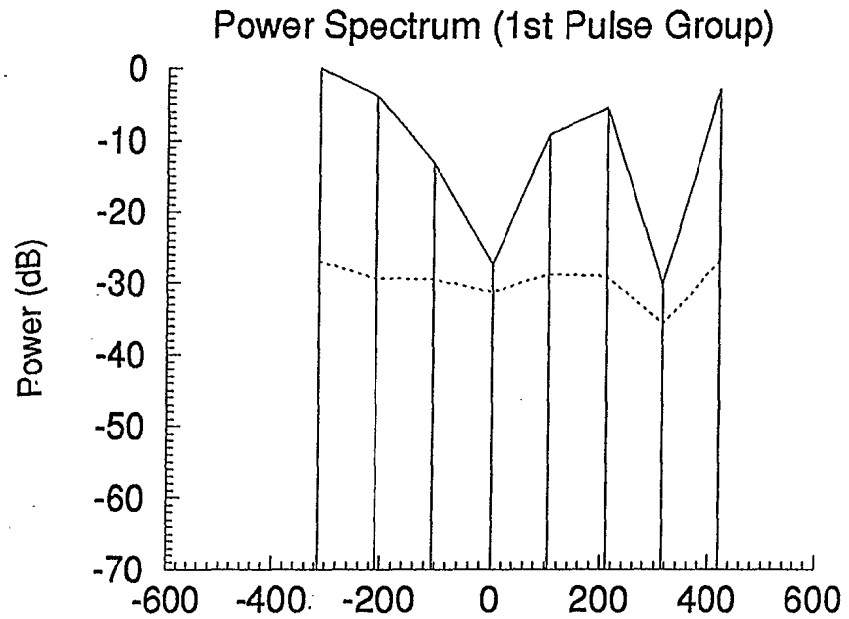

Figure 20a. Doppler Shift in Hertz (8 pulses).

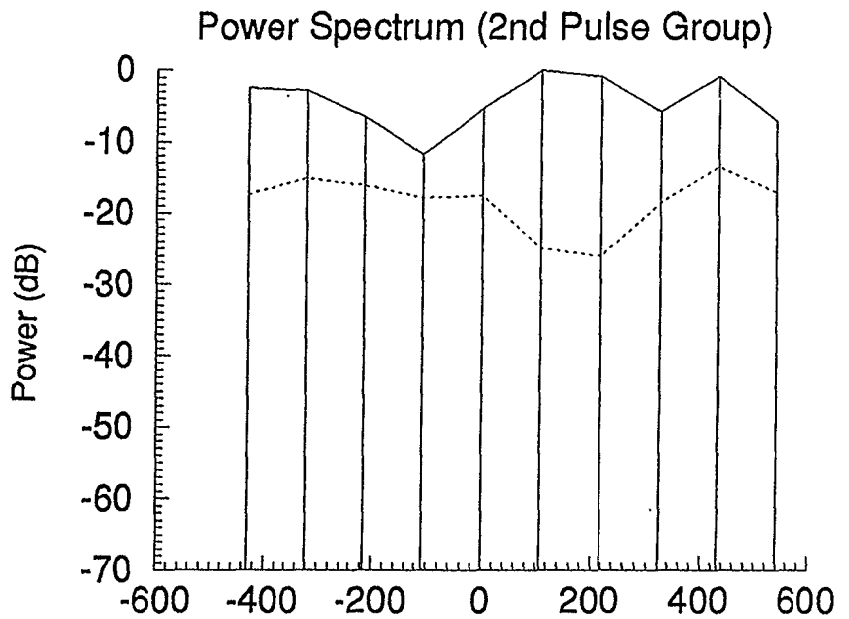

Figure 20b. Doppler Shift in Hertz (10 pulses).

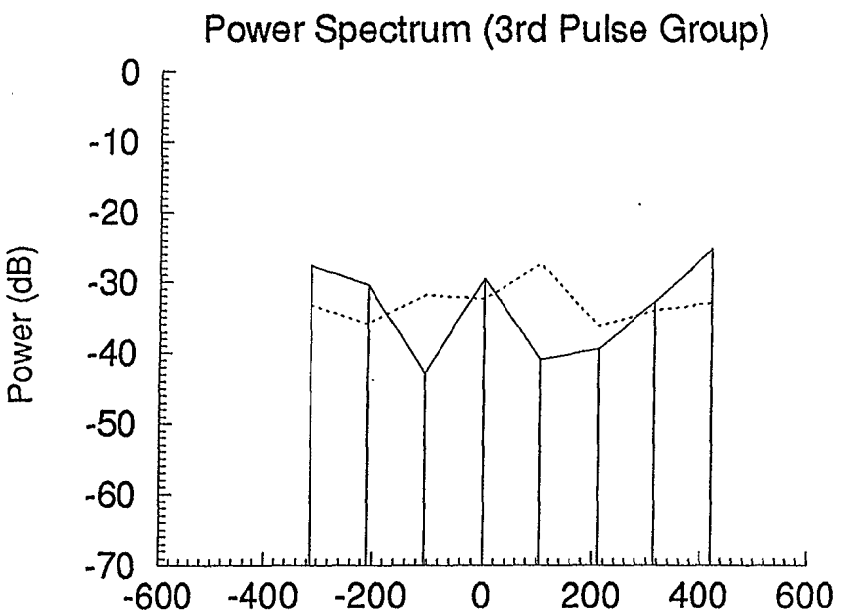

Figure 20c. Doppler Shift in Hertz (8 pulses).

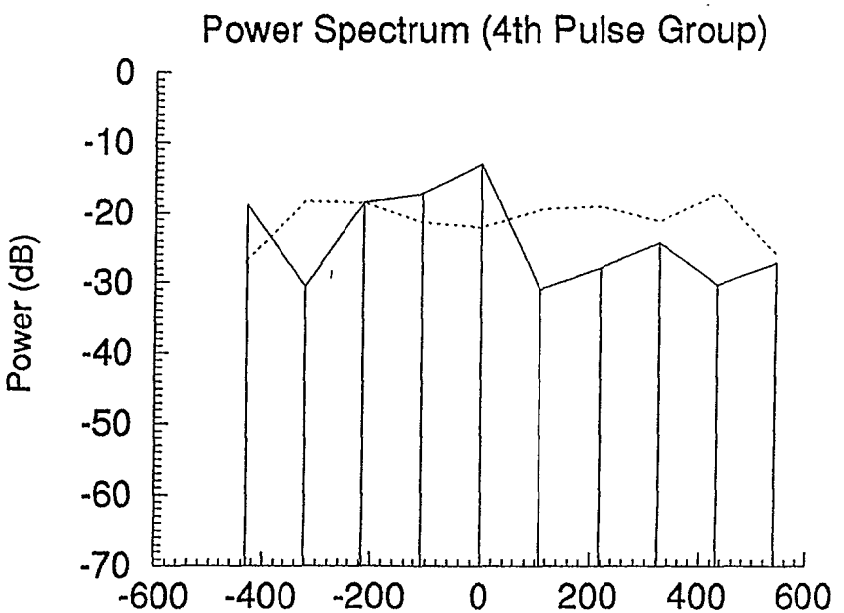

Figure 20d. Doppler Shift in Hertz (10 pulses).

Doppler Filter Amplitudes, Scan 6 (target) and 8 (noise), Range Cell #108

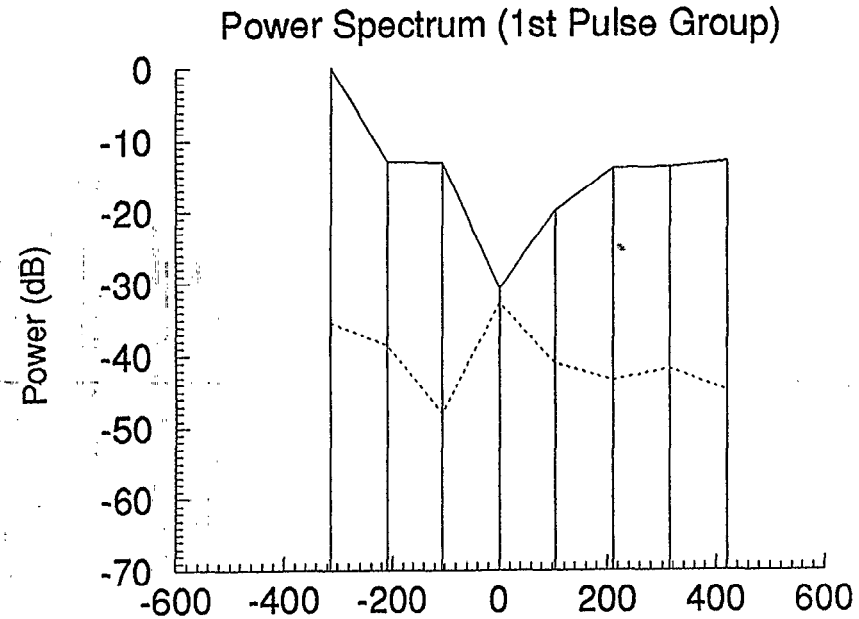

Figure 21a. Doppler Shift in Hertz (8 pulses).

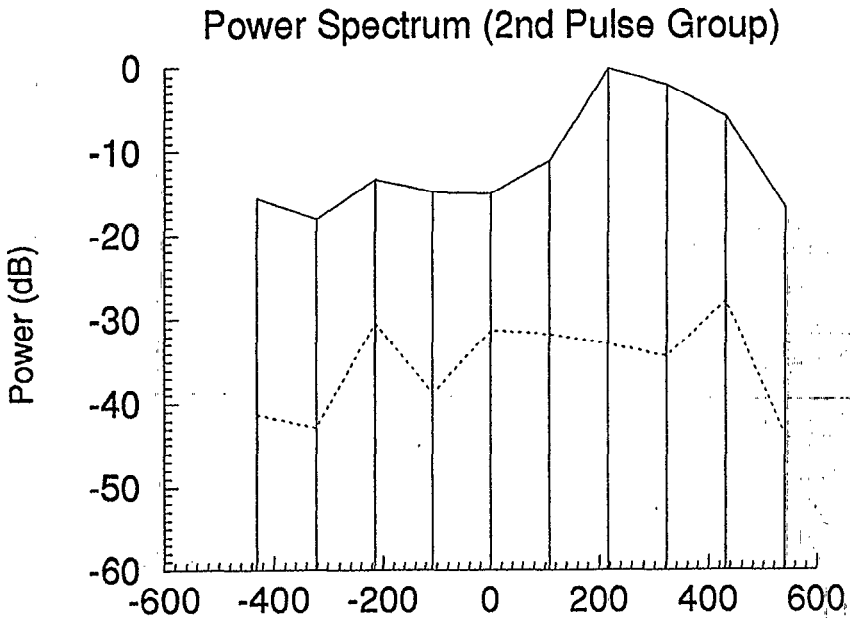

Figure 21b. Doppler Shift in Hertz (10 pulses).

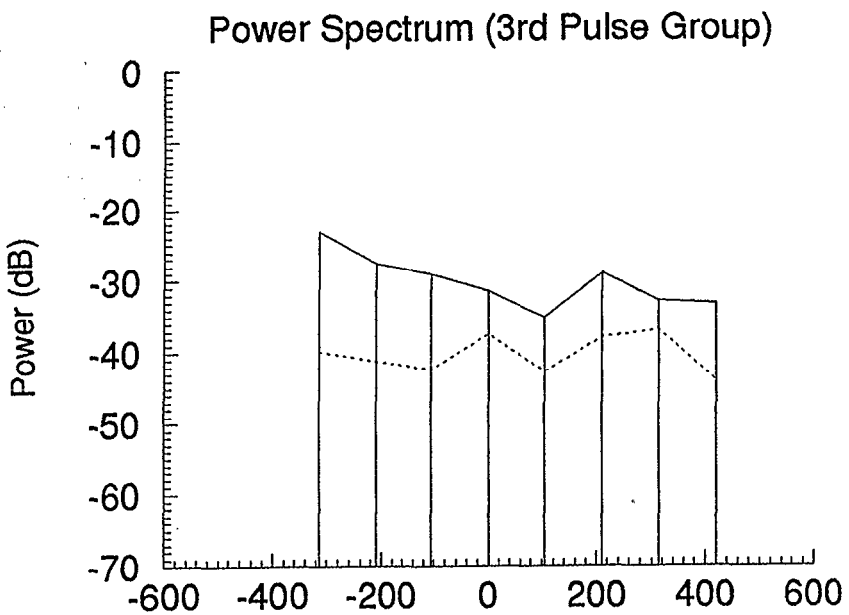

Figure 21c. Doppler Shift in Hertz (8 pulses).

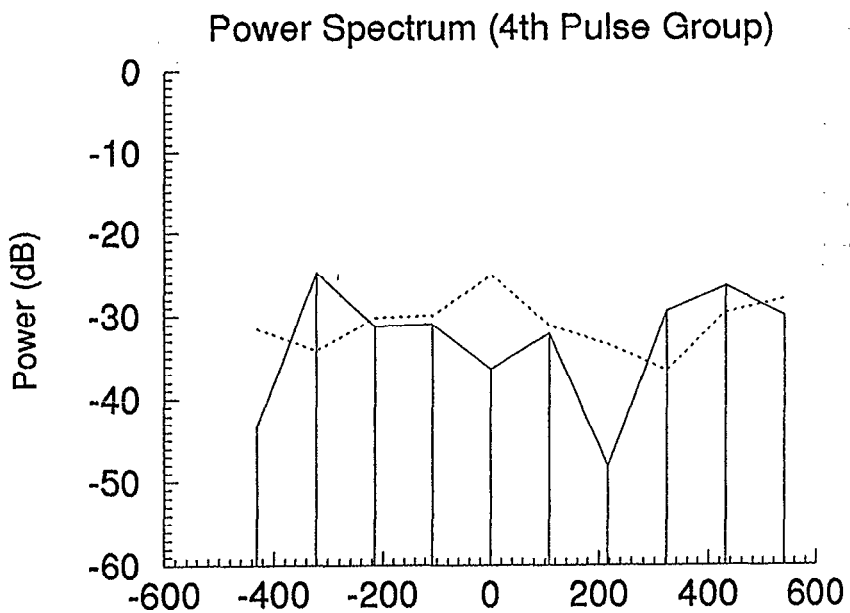

Figure 21d. Doppler Shift in Hertz (10 pulses).

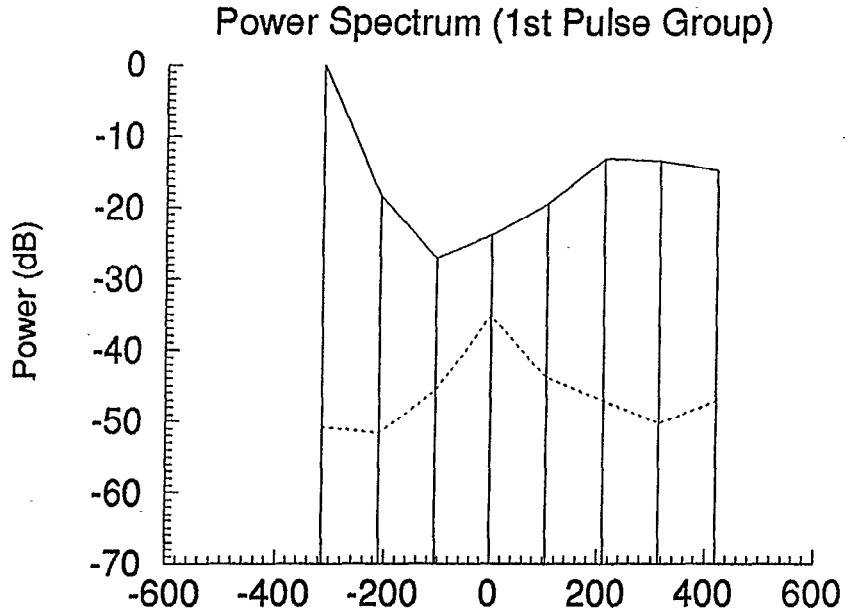

Figure 22a. Doppler Shift in Hertz (8 pulses).

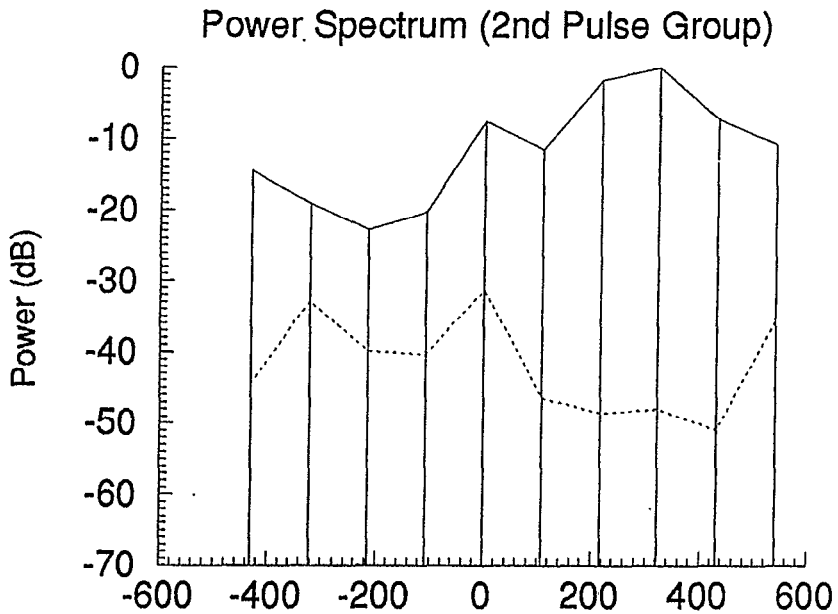

Figure 22b. Doppler Shift in Hertz (10 pulses).

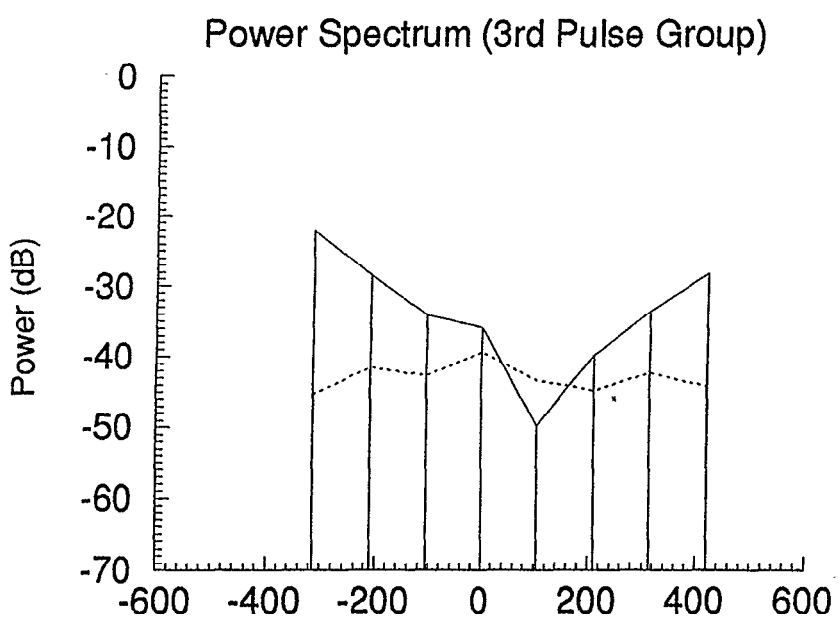

Figure 22c. Doppler Shift in Hertz (8 pulses).

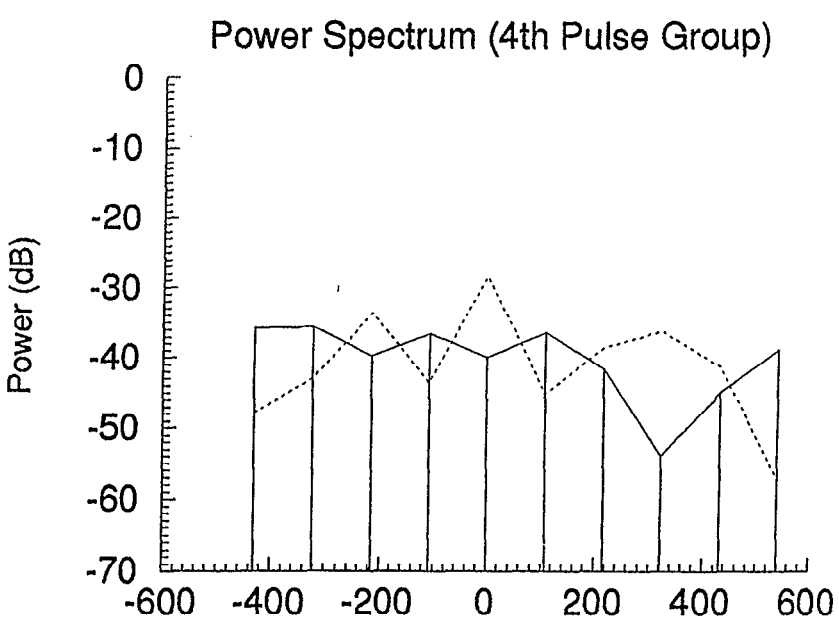

Figure 22d. Doppler Shift in Hertz (10 pulses).

4. CONCLUSION AND RECOMMENDATIONS

The Gilfillan/Thomson solid state radar system has impressive stability and time sidelobe performance. The field tests show an instability residue capability nearly an order of magnitude lower than is claimed in current FAA radar systems. However, to take full advantage of this improved performance, the radar signal processor must remove the deterministic effects of the transmitter's thermal time constants during staggered PRF operation. Finally, depending on the details of a future system implementation, antenna scan modulation may limit the radar's ultimate clutter rejection capability.

The very low time sidelobe performance measured during the demonstration shows much promise for target and weather detection without range smearing or other undesired artifacts from the compression process. First-order simulations of weather detection using a Thomson-like compressed waveform have shown that these low sidelobe levels, if maintained for a complex extended target, can provide adequate weather detection. However, a doppler-varying high-reflectivity gradient weather event (like a thunderstorm cell) could cause smeared responses due to the radar's integrated sidelobe levels. In addition, at close ranges (where airport runways are located), the short pulse waveform may not have enough energy to detect low-reflectivity events such as gust fronts or dry microbursts. No weather data addressing these issues were taken during the FAATC demonstration. In addition, the radar signal processor must compensate for the (deterministic) staggered PRF step phase changes in order to maintain radar waveform performance across PRIs.

The FAATC ASR-9 radio frequency and processor hardware were not optimum for a complete demonstration of the solid state radar's performance capabilities. As mentioned above, more thorough demonstration, test, and analysis require optimized, independent high/low beam switching, independent STC's for the two waveform channels, and much more extensive, high dynamic range data recording and realtime display capabilities. From the very limited data available from the FAATC demonstration, however, the radar's raw target detection capability appears to match its predicted performance.

The FAATC solid state radar demonstration marks a promising milestone in advancing air traffic control radar technology. Serious questions remain, however, concerning the new technology's performance in severe and low-reflectivity weather, in extended clutter, and in a real-world interference environment. In addition, algorithms for optimization of the radar hardware configuration, the STC, the CFAR, and transmitter thermal effects compensation all need to be developed and tested. The recommended path for such testing and development is a combination of detailed simulation, extensive hardware-in-the-loop testing, and stressing field measurement with weather and target truthing and thorough instrumentation. Following such a set of recommendations will ensure that solid state technology feeds into TASS or other radar procurements with minimum technological risk, while maximizing the potential maintenance and performance benefits offered by solid state radar.

APPENDIX

Essential Technical Characteristics

Parameter	Measured Value	Notes
Output power	19 kW short pulse 22 kW long pulse	
Pulse widths	.85 uS short pulse 74 uS long pulse	
Output power degradation	< 0.5 dB with two failed RF output modules	
Rcvr noise figure	1.46 dB	
Rcvr dynamic range	78.6 dB long pulse 61.8 dB short pulse	MDS to approx. 1 dB compression 14 bit A/D; 18 bit I & Q after pulse compression
I & Q image rejection	Avg. ~60 dB	Digital I & Q Generation
Time sidelobes	-55 to -51 dB peak	At doppler shifts up to the equivalent to a 130 m/sec target speed, with or without delay, with transmitter compensation, no STC. Independent of cold module swaps.
System stability	61 to 62 dB	Field measurement with or without pulse stagger; pulse stagger requires pulse group amplitude compensation

REFERENCES

[1] Healy, Thomas A. and Richard L. Ferranti. "ASR Solid State Transmitter Demonstration Final Report," FAA Technical Center, Atlantic City Airport, NJ 08405, Final Draft of December 27, 1993.

[2] Hansen, J. W. et al., Systems Applications of Communications TWTAs, (Hughes Aircart Company, Electron Dynamics Division, August 1982), p. 36.